

JENA LASER CONFERENCE

#JLT15

CONFERENCE PROCEEDINGS

Lasers and processes for digital manufacturing technology

JENA, NOV 4+5 26

LASERTAGUNG-JENA.DE

OptoNet e. V. (Publisher)

15th Jena Laser Conference

Lasers and processes for digital manufacturing technology

Topics

Laser Beam Joining Additive Manufacturing and Industrial Materials Processing

Biophotonics Fluorescence Microscopy and Optical Manipulation

Laser Processing for Microstructuring Glass and Functional Surfaces

Laser Beam Sources Beam Shaping and Beam Characterization

Photonics for Quantum High Power and Integrated Systems

Optical Components Coatings and Freeform Optics

Event Partners

OptoNet e. V.
University of Applied Sciences Jena
Institute of Applied Physics Friedrich Schiller University Jena

Verlag Ernst-Abbe-Hochschule Jena | 2026

Bibliographic information of the German National Library
The German National Library lists this publication in the German National Bibliography; detailed data is available on the Internet at https://portal.dnb.de/.

Publisher: OptoNet e.V.

eISBN (PDF) 978-3-932886-56-0

© 2026 Verlag Ernst-Abbe-Hochschule Jena, Jena, Germany

Reproduction, even in part, is only permitted with the permission of the University of Applied Sciences Jena.

University of Applied Sciences Jena
Carl-Zeiss-Promenade 2
07745 Jena
Germany

Typesetting/Layout: Manuela Lohse, ML Verlagswesen, Jena, Germany
Proofreading: The contributions and posters were set as manuscripts.

Program Commission

Prof. Dr. Hartmut Bartelt	Leibniz Institute of Photonic Technology e. V.
Prof. Dr.-Ing. habil. Jean-Pierre Bergmann	Ilmenau University of Technology
Prof. Dr.-Ing. Jens Bliedtner	Ernst Abbe University of Applied Sciences Jena
Dr. Felix Dreisow	SCHOTT Technical Solutions GmbH
Prof. Dr. rer. nat. habil. Alexander Horn	Mittweida University of Applied Sciences
Thomas Hucke	Linde AG, Linde Gas Division
Dr.-Ing. Simon Jahn	ifw Jena | Günter-Köhler-Institute for Joining Technology and Materials Testing
Prof. Dr. Stefan Nolte	Friedrich Schiller University Jena
Prof. Dr. rer. nat. habil. Andreas Tünnermann	Fraunhofer Institute for Applied Optics and Precision Engineering IOF

Sponsors

We would like to thank our sponsors and supporters for organizing and conducting the conference.

Platinum Sponsor

JENOPTIK

MORE LIGHT

Gold Sponsors

LASER COMPONENTS

TRUMPF

Silver Sponsors

Edmund optics | worldwide

EurA

excelitas

JAT JENAER ANTRIEBSTECHNIK

LIGHT CONVERSION

mks | Ophir

ROBUST AO

PRIMES

TOPAG

Program Commission **4**
Sponsors **4**

Session I A – Laser Beam Joining Additive Manufacturing and Industrial Materials Processing

Single-material beverage packaging, and what the CO_2-laser has to do with it 6

The influence of variable power distributions on process dynamics during laser welding of copper and aluminum using concentric intensity distributions 7

Grain Refinement in Femtosecond Laser Powder Bed Fusion of Zirconia 8

Breakthrough in laser drilling technology: Taper-free machining of technical ceramics for sensor applications 9

Session I B – Biophotonics Fluorescence Microscopy and Optical Manipulation

Laser tweezers as force sensors in living biological systems 10

Plug-and-Play kHz Laser Control System for Advanced Fluorescence Microscopy 11

From FRET-Guided RNA 3D Structures to Conformational Ensemble 12

Laser Engine for High-Speed Multimodal Fluorescence Microscopy 13

Session II A – Laser Processing for Microstructuring Glass and Functional Surfaces

Excimer laser micro structuring setup using a micro mirror array as programmable mask 14

Image-Based Geometric Analysis of Laser-Structured Through-Glass Vias (TGVs) in Borofloat Glass (BF33) 15

Selective ablation of silver, aluminum, and gold mirrors with protec-tive dielectric coating 16

Determining the influence of a protective dielectric coating on the ablation of metallic mirrors 17

Session II B – Laser Beam Sources Beam Shaping and Beam Characterization

Enabling Diverse Laser Applications with Customized Photonic Solutions 18

Overcoming Rayleigh – Characterization of ring-shaped laser beams in a systematic way 19

Focusing ultrashort UV pulses with industrial objectives: Onset and impact of spatiotemporal effects 20

Dynamic beam shaping with a multicore-fiber-based, high-power, femtosecond CPA laser system 21

Session III A – Photonics for Quantum High Power and Integrated Systems

Low-loss femtosecond-written waveguides for co-packaged optics 22

The Femtosecond Laser as a Versatile Tool for Fabricating All-Glass Atomic Vapor Cells for Quantum Applications 23

High-Power Diode Laser Pump Modules for Solid State Laser-Driven Fusion Reactors 24

Session III B – Optical Components Coatings and Freeform Optics

Tailored nanostructured AR coatings for high-intensity laser systems 25

Cr(VI)-Free Black Electroless Nickel Coatings for Optical and Laser Applications 26

Direct Ultrashort Pulsed Laser Welding of Zerodur to Stainless Steel 27

Posters **28**
Author directory **38**

Günter-Köhler-Institut
für Fügetechnik und
Werkstoffprüfung

ifw Jena

Single-material beverage packaging, and what the CO_2-laser has to do with it

Thomas Schmidt, Susanne Kasch – ifw Jena GmbH

Tobias Naumann – Husky Technoligies™

Currently, closures for typical PET beverage containers are made of polyethylene or polypropylene. These materials offer the necessary properties to meet the demanding requirements of a beverage closure. These include adequate sealing, compressive strength, impact resistance and temperature resistance. The disadvantage becomes apparent during recycling: PET can be recycled back into food-grade material, whereas PE or PP cannot. This means the cap and bottle must be laboriously separated before recycling.

The necessary separation of cap and bottle can be completely avoided if both are made of the same material. If PET is also used for the closure, a single-material beverage container is created, which offers significantly higher purity, thereby enabling easier recycling and a higher recycling rate. The regulation regarding the tethered caps to the bottle also then takes on its full significance. However, due to the material properties of PE and PP differing from those of PET, the previous method for the initial sealing of the bottles cannot be used. The bridges connecting the TEB (Tamper-Evident Band) to the cap would break during the mechanical sealing of the bottle.

With this development, ifw Jena and Husky Technologies have found a new and innovative way to implement the tamper-evident feature even with PET caps. This is where the CO_2 laser comes into play, molding the TEB onto the bottle. Based on these investigations, an initial system prototype was developed, which successfully demonstrated the functionality on the production line. As a result, a second system was developed capable of handling a bottle throughput of up to 45,000 units per hour. Currently, the market launch is underway, along with further development for bottle throughputs of 100,000 units per hour and higher.

This article presents the development work on forming the TEB using laser technology, ranging from individual bottles to high-speed applications. Starting from the initial idea and exploring various system concepts, it offers a view into the future of beverage packaging.

The influence of variable power distributions on process dynamics during laser welding of copper and aluminum using concentric intensity distributions

Authors: J. Scheffler, C. Diegel, L. Schmidt, J. P. Bergmann

Institute: Technische Universität Ilmenau, Fachgebiet Fertigungstechnik

E-Mail: jonas.scheffler@tu-ilmenau.de

Telephone: +49 3677 69-3847

Address: Gustav-Kirchhoff-Platz 2, 98693 Ilmenau

The increasing use of copper and aluminum materials in electric vehicle applications places high demands on reliable and efficient joining processes. Laser welding offers great potential due to its high energy densities and process speeds. However, the use of these materials is limited by low absorption and the high dynamics of the keyhole and surrounding melt pool. This frequently leads to weld defects such as porosity and spatters.

Using concentric intensity distributions in the form of core-ring beam profiles is a promising approach to reduce the formation of weld defects. Previous studies have primarily assessed their influence on weld quality, whilst a physically sound understanding of the underlying effects is still lacking.

This study therefore adopts a physics-based approach that focuses on the interactions between energy input, keyhole dynamics and melt behavior. To this end, the ring power is systematically varied whilst keeping the core power constant, in order to specifically investigate the influence of radial energy distribution.

The analysis is carried out using high-speed imaging to capture the keyhole dynamics and spatter formation. This involves determining characteristic parameters such as spatter rate, detachment angle and temporal fluctuations in keyhole geometry. In addition, metallographic sections and computed tomography scans are used to assess weld geometry and porosity.

The results show that increasing ring powers lead to a significant change in keyhole dynamics, which can reduce spatter formation significantly. The observed effects are attributed to alternative energy distribution and a change in the pressure conditions within the keyhole. This work thus advances the physical understanding of the mechanisms underlying concentric intensity distributions in laser welding of copper and aluminum.

Grain Refinement in Femtosecond Laser Powder Bed Fusion of Zirconia

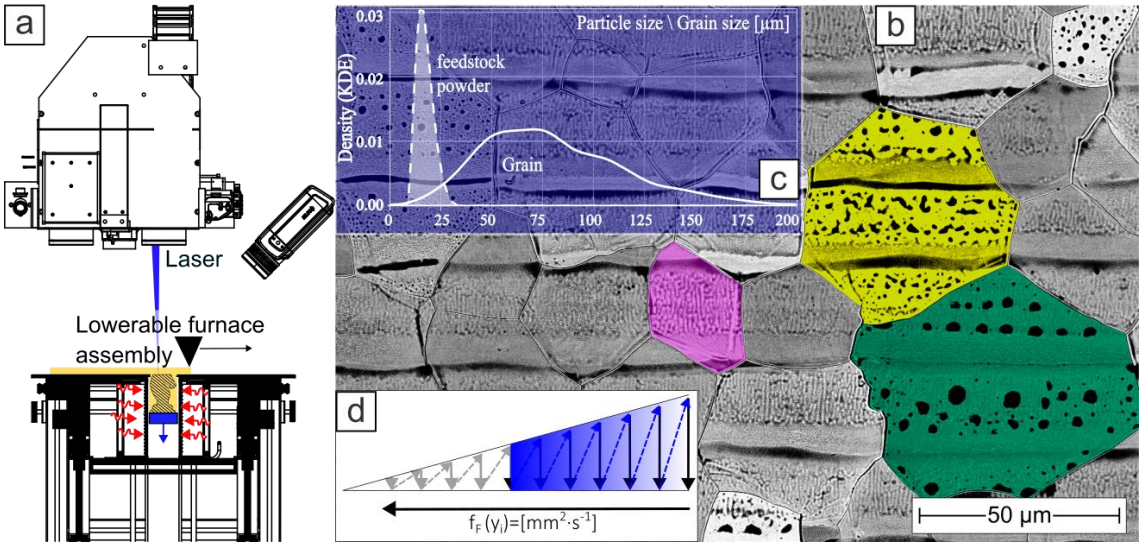
Markus Kühn[1], Sarah Kaden[1], Andrea Barz[1], Daniel Störzner[2], Jens Bliedtner[1], Andrés Fabián Lasagni[3,4]

[1] Ernst-Abbe-Hochschule Jena, Bliedtner Research Group, Germany
[2] LCP Laser-Cut-Processing GmbH, Hermsdorf, Germany
[3] Technische Universität Dresden, Germany
[4] Fraunhofer IWS, Dresden, Germany

Abstract

Controlling grain growth is essential for producing homogeneous zirconia microstructures by laser powder bed fusion. We investigate how laser power, scan speed, defocus and pulse repetition rate affect surface homogeneity and grain-size distributions in binder-free 8 mol% yttria-stabilized zirconia (8YSZ) single layers processed with 220 fs pulses at 1030 nm.

The setup (panel a) uses triangular scans of varying vector length (panel d) to assess heat accumulation. Optical surface analysis, infrared thermography and a reduced heat-conduction model complement SEM grain segmentation (panel b). More than 4,000 grains are evaluated statistically, with particle and grain size distributions compared in panel c.



Femtosecond PBF-LB of 8YSZ: (a) setup, (b) SEM image with segmented grains, (c) particle and grain size distributions, and (d) triangular scan strategy.

Raising scan speed from 200 to 400 – 500 mm/s reduces the mean equivalent grain diameter from 51.8 to approximately 40 µm and narrows its distribution. Increasing positive defocus from 5 to 15 mm reduces the distribution's full width at half maximum from about 56 to 27 µm. An intermediate repetition rate of 8 MHz yields the narrowest distribution among the frequencies evaluated for grain size. Within the established process window, laser power has a weaker effect on grain size. These trends are consistent with shorter residence times at high temperature limiting grain coarsening. The results identify scan strategy and laser parameters as tools for tailoring grain size in zirconia layers without binders or absorptive additives.

Presenting author and contact

Markus Kühn | Research Associate
Room 04.00.47, Carl-Zeiss-Promenade 2, 07745 Jena, Germany
Tel.: +49 3641 205 9719 | Email: markus.kuehn@eah-jena.de

LCP Laser-Cut-Processing GmbH
Heinrich-Hertz-Str. 16
07629 Hermsdorf
Mr. Carl Stelzig
+49 36601 9327-48
carl.stelzig@lcpgmbh.de

Ein Beitrag aus dem Forschungsprojekt SAPHIR

Headline

[de] Durchbruch in der Laserbohrtechnologie: Taperfreie Bearbeitung von technischen Keramiken für Sensoranwendungen

[en] Breakthrough in laser drilling technology: Taper-free machining of technical ceramics for sensor applications

Abstract

[de] Technische Keramik ist aus modernen Hochleistungsanwendungen nicht mehr wegzudenken – ob in der Sensorik, Medizintechnik oder Mikroelektronik. Doch gerade beim Laserbohren dieser spröden Werkstoffe kommen herkömmliche Bohrprozesse mit UKP-Lasern an ihre Grenzen. Durch die Ausbildung des Taper werden insbesondere Tieflochbohrungen meist nur mit konischen Schnittkanten erzeugt. Die Prozessgrenzen, welche sich beim Mikrobohren von dünnen Folien nur geringfügig auswirken, führen bei höheren Materialstärken zu einer deutlichen Einschränkung der Bearbeitung.

Dieser Artikel befasst sich mit der Weiterentwicklung des UKP-Laserbohrens mit Trepanieroptik, welche im Rahmen des Förderprojektes SAPHIR umgesetzt wurde. Innerhalb des Projektes wurde der Bohrprozess optimiert sowie die Strahlführung und -formung angepasst um das Laserbohren von hart-spröden Werkstoffen mit Trepanieroptik entscheidend zu verbessern. Durch die Modifikation der Anlagentechnik und Optimierung des Bohrprozesses, gelang ein entscheidender Durchbruch: taperfreie, hochpräzise Bohrungen, die nicht nur die Qualität steigern, sondern auch neue Designfreiheiten eröffnen. Zudem können nun auch dickere Materialien schnell und effizient laserbearbeitet werden.

[en] Technical ceramics have become a key part of modern high-performance applications—whether in sensor technology, medical technology, or microelectronics. Conventional drilling processes using UKP lasers, in particular, reach their limits when it comes to laser drilling of these brittle materials. Due to the formation of the taper, deep-hole drilling is typically performed with only conical cutting edges. While process limits have only a minor impact during micro-drilling of thin films, they significantly restrict machining capabilities when dealing with thicker materials.

This article discusses the further development of UKP laser drilling using trepanning optics, which was carried out as part of the SAPHIR research project. As part of the project, the drilling process was optimized and the beam guidance and shaping were adjusted to significantly improve laser drilling of hard, brittle materials using trepanning optics. We made a major leap forward by modifying the equipment and optimizing the drilling process: taper-free, high-precision holes that not only improve quality but also open up new design possibilities. On top of that, thicker materials can now also be laser-processed quickly and efficiently.

Laser tweezers as force sensors in living biological systems

Maria Dienerowitz, Ernst-Abbe-Hochschule Jena / University of Applied Sciences Jena

Laser tweezers are an optical tool to non-invasively trap, manipulate and probe microscopic objects with nanometre precision and pico-Newton force resolution. While they are widely used in biophysics, their underlying working principle is closely connected to laser technology. A tightly focused laser beam creates a calibrated force sensor whose performance depends on beam quality, aberration control and beam shaping. This contribution will introduce optical tweezers from a laser-applications perspective and explain how forces can be measured between cells or particles trapped in an optical potential.

The major advantage that makes optical tweezers highly suitable for biological interaction studies is their non-invasive, mechanical-contact-free nature. In bacterial systems, optically trapped cells can be positioned relative to each other to probe forces during cell-cell approach, providing access to processes relevant to aggregation and early biofilm formation. In ligand-receptor studies, functionalized trapped particles can be brought into contact with living cells, allowing binding and rupture events to be quantified through changes in particle position.

Holographic beam shaping enables this type of force spectroscopy by generating multiple digitally controlled traps and allowong the controlled positioning of several objects in three dimensions. It is also crucial for optimising the focus, and thus trap quality, deeper inside biological samples, where aberrations and non-ideal focusing conditions deteriorate the shape of the optical potential. The presentation will combine an accessible introduction to optical force measurements with selected examples from interdisciplinary collaborative work. It will highlight optical tweezers as a versatile laser application at the interface of beam shaping, microscopy and quantitative life-science measurements.

Plug-and-Play kHz Laser Control System for Advanced Fluorescence Microscopy

Josephine Meitzner, Paul Lehmann*, Sascha Klötzer, Richard Börner*

Laserinstitut Hochschule Mittweida | Mittweida University of Applied Sciences

**Equally contributing authors*
J. Meitzner and P. Lehmann are equally contributing authors.

Referent:
Paul Lehmann
+49 3727 581868
lehmann6@hs-mittweida.de
Laserinstitut Hochschule Mittweida, Technikumplatz 17, 09648 Mittweida

Single-molecule microscopy utilizing alternating laser excitation (ALEX) is an established method for the characterization of biomolecules. However, existing laser control systems are often costly and OEM-specific, limiting flexibility in customized microscopy environments.

To overcome these limitations, we developed an independent, user-friendly laser control approach based on a microcontroller architecture capable of managing up to four individual laser sources. The system is specifically designed for advanced fluorescence microscopy, allowing users to implement preconfigured as well as fully customizable triggering schemes via an intuitive Graphical User Interface (GUI). This enables complex illumination modes such as ALEX for Total Internal Reflection Fluorescence (TIRF) and confocal fluorescence microscopy assays.

The developed solution supports both external hardware triggering and flexible frequency or pulse-width modulation (PWM), achieving pulse durations from 20 µs to 10 s with pulse repetition rates reaching up to 50 kHz. The approach is compatible with any laser source that can be externally modulated via standard TTL signals, providing a highly adaptable and ready-to-use solution for integrated optical systems in the life sciences and beyond.

Richard Börner, Hochschule Mittweida

FROM FRET-GUIDED RNA 3D STRUCTURES TO CONFORMATIONAL ENSEMBLE

RNA molecules often populate multiple conformational states, yet integrative modelling approaches have traditionally focused on identifying single structural models that satisfy experimental restraints. Here, I will discuss how Förster resonance energy transfer (FRET) can be used not only to guide and validate individual RNA 3D structures, but also to select structural collections that better represent conformational heterogeneity.

We combine ensemble and single-molecule FRET experiments with RNA 3D structure prediction, accessible-contact-volume dye modelling, and FRET-assisted modelling pipelines. The approach is illustrated using ribosomal RNA tetraloop-receptor interactions, in which a GAAA tetraloop binds its receptor in a metal-ion-dependent manner. This model system provides a stringent test case because it combines a well-defined tertiary RNA contact with experimentally accessible conformational states and distance restraints.

Building on our previous work on FRET-guided modelling and FRET-guided selection of RNA 3D structures, I will show how experimental FRET restraints can discriminate between predicted structures, identify compatible subsets from large structure pools, and support the transition from single best-fit models towards conformational ensembles. These structure collections provide a more realistic description of RNA molecules that fluctuate between related, experimentally observable conformations.

Finally, I will outline how single-molecule FRET data may extend this concept further by linking selected conformational states into folding trajectories. While the full integration of kinetic and dynamic single-molecule information into structural modelling remains an open challenge, it offers a promising route towards experimentally grounded, FRET-guided descriptions of RNA folding landscapes. Together, these developments establish FRET-guided integrative modelling as a bridge between RNA structure prediction, experimental biophysics, and future data-driven modelling of RNA conformational dynamics.

Laser Engine for High-Speed Multimodal Fluorescence Microscopy

Uniform laser illumination is key to further improving advanced fluorescence microscopy and single-molecule imaging methods. At the same time, modern microscopy platforms increasingly require multiple excitation modalities, including broad wavelength coverage, high-speed laser switching, and picosecond-pulsed excitation, which leads to complex laser illumination setups.

We present an all-in-one versatile laser engine designed for high-speed multimodal fluorescence microscopy. The system combines multi-wavelength flat top-hat illumination, high-speed switchable lasers, and picosecond pulsed lasers for fluorescence lifetime applications within a single integrated platform. It provides flat-field illumination with up to 97% homogeneity at 10 µs exposure time, making it suitable for fast imaging applications and serving as an alternative to classical beam-shaping approaches. The system supports picosecond laser operation at repetition rates up to 100 MHz and high-speed switching lasers up to 50 MHz. It enables switching between excitation schemes, including super-resolution imaging, TIRF, and fluorescence lifetime imaging microscopy (FLIM).

The platform currently supports up to six excitation wavelengths and provides a cost-efficient alternative to comparable commercially available systems while maintaining optical output power of up to 1.5 W per wavelength. In addition, the system enables advanced biophysical methods such as parallelized single-molecule detection based on zero-mode waveguides and wide-field fluorescence lifetime imaging.

The laser engine has been transferred into a commercially available product platform for advanced fluorescence microscopy and bioimaging instrumentation. The product provides an user-friendly, fully integrated solution for next-generation multimodal microscopy in both research and industrial environments.

Excimer laser micro structuring setup using a micro mirror array as programmable mask

Sebastian Buettner[1], Jan-Uwe Schmidt[2], Markus Hilmes[2] and Steffen Weissmantel[1]

[1]*Laserinstitut Hochschule Mittweida (LHM), University of Applied Sciences Mittweida, Germany*

[2]*Fraunhofer Institute for Photonic Microsystems (IPMS)*

Contact: buettner@hs-mittweida.de

Keywords: micro structuring, micro-optics, excimer laser, micro mirror array, micro lens array, Fresnel lenses

Spatial light modulators (SLMs) such as digital micro mirror devices (DMDs), liquid crystal on silicon (LCoS), liquid crystal displays (LCDs) or grating light valves (GLVs) are well used in laser technology and light processing such as maskless lithography [1-7]. LCOS SLMs are restricted to the NIR-VIS spectral range. Different variants of DMD and GLV operate in the NIR, VIS and UV. At DUV wavelengths of < 200 nm, to our knowledge, only customized micro mirror arrays (MMAs) developed at Fraunhofer IPMS are usable.

At the LHM, we developed and investigated different methods for micro-optics generation using excimer lasers in recent years. By using specially shaped apertures and amplitude masks we could generate several different micro-optics in transparent materials. To overcome the shortcomings of these classical mask projection methods, we built the first DUV laser micro structuring setup using an MMA as programmable reflective mask. The used MMA developed and provided by Fraunhofer IPMS consists of 2048 x 512 micro mirrors. The MMA currently provides a frame rate of up to 1 kHz. The individually addressed mirrors have 16 µm pitch and offer continuous tilt control. The mirror reflectance is optimized for 193 nm wavelength. As laser source we use the Coherent ExciStar Industrial with max. pulse energy of 15 mJ at 10.5 ns pulse duration and max. frequency of 200 Hz. The short wavelength of 193 nm ($E_p = 6.43\ eV$) and the high fluence in the image plane of the system is sufficient for the excitation and ablation of borosilicate glass ($E_g \sim 3.2\ eV$ / $H_{th} \sim 0.4\ J/cm^2$). With this setup we can generate arbitrary phase profiles and virtually all kinds of micro-optics in borosilicate glass within few milliseconds for each field of view. For demonstration of the capabilities of our setup, we generated an 8-level Fresnel lens array with 10,000 identical hexagonal lenslets in less < 20 min (Fig. 1). The measurements in Fig. 2 show that the function of the lenslets is almost diffraction limited ($d_{Airy} = 7{,}03\ \mu m$ / $d_{Limit} = 6.21 \mu m$).

Currently, we use binary mask patterns to generate different kinds of microstructures. In further investigations, we want to optimize the whole imaging system for gray scale ablation and stabilize the laser pulse energy within a burst to achieve machining accuracy in the lower nanometer range. Finally, we are looking forward to scaling the process up to 1 kHz laser pulse frequency to reach an area processing rate in the range of cm²/min.



Fig. 1: Micro lens array in Borosilicate glass N-BK7.

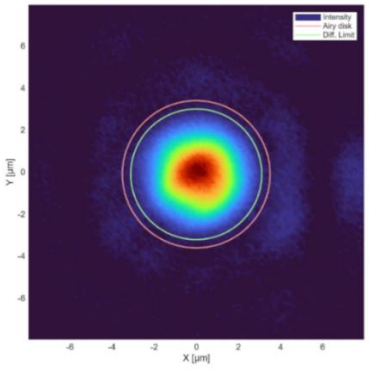


Fig. 2: Intensity distribution in the focus of a lenslet and measured / diffr. limited Airy disk.

1. Ljungblad, U. B.; Askebjer, P.; Karlin, T. et al. (2005), Proc. SPIE Vol. 5721.
2. Gehner, A.; Wildenhain, M.; Neumann, H.; Knobbe, J. et al. (2006), Proc. SPIE 6113.
3. Dauderstädt, U.; Askebjer, P.; Björnängen, P. et al. (2009), Proc. SPIE 7208.
4. Schmidt, J. U.; Dauderstaedt, U.; Duerr, P. et al. (2014), Proc. SPIE Vol. 8977.
5. Klerks, Tobias; Eifel, Stephan (2016), Proc. LANE 2016.
6. Zhong, K.; Zhang, H.; Gao, Y. (2017), Optik 142, pp. 243-248.
7. Huang, S.; Li, M.; Shen, L.; et al. (2018), Optics & Laser Technology 100, pp. 298-303.
8. Sandner, T., Schmidt, J.U., Schenk, H. et al. (2005), Proc. SPIE 5721.
9. Schmidt, J.-U.; Bring, M., Heber, J. et al. (2010), Proc. SPIE 7716, 77162L.

The results presented in this publication are based on work supported by the Federal Ministry of Finance, Technology and Resources (BMFTR) under the VIP+ funding program for the project MMA(q)opt. The authors gratefully acknowledge financial support.

Bundesministerium für Forschung, Technologie und Raumfahrt

Image-Based Geometric Analysis of Laser-Structured Through-Glass Vias (TGVs) in Borofloat Glass (BF33)

Abstract

Current megatrends in artificial intelligence (AI) continue to push the boundaries of technology. Higher computing performance and increasing heat generation are driving the need for innovative advanced packaging solutions in the semiconductor industry. One promising approach is the implementation of a high density of through-glass vias (TGVs) on panel formats of up to 600 mm × 600 mm. For this purpose, localized modifications are introduced into the glass substrate by ultrashort pulse laser processing and subsequently enlarged to the target diameter by wet-chemical etching. The resulting TGV properties, such as diameter, roundness, and shape, strongly depend on the selected laser parameters.

This paper presents an application-oriented and reproducible methodology for the evaluation of TGVs. For this purpose, microscope images of the top and bottom sides of structured samples are acquired under selected illumination conditions and analyzed by means of digital image processing. The implementation is carried out in a Python environment using the Open Source Computer Vision Library (OpenCV). A Gaussian fit is used to determine the circle center as well as additional parameters relevant for the evaluation, including the average diameter and the maximum and minimum diameters. In addition, process-related artifacts such as edge chipping can be identified. The methodology is used to analyze the influence of various parameters, including pulse energy, focus position, pulse duration, and burst mode, on properties such as diameter tolerance, roundness, and process stability, and to derive suitable process windows.

In summary, a robust approach for the evaluation of laser-induced TGVs is presented that enables targeted control of TGV properties in this technologically highly relevant and emerging process field of semiconductor manufacturing.

Keywords

TGV, BF33, ultrashort pulse laser, roundness, pulse energy, focus position, etching, image processing, semiconductor industry

Selective ablation of silver, aluminum, and gold mirrors with protective dielectric coating

Vincent Rupf[1], Markus Olbrich[1], Andy Engel[1], Robert Schmidt[2], Jens Bliedtner[2], and Alexander Horn[1]
[1]Laserinstitut Hochschule Mittweida, Technikumplatz 17, 09648 Mittweida
[2]Ernst-Abbe-Hochschule Jena, Carl-Zeiss-Promenade 2, 07745 Jena

This study fundamentally investigates the selective removal of multilayer coatings from optical components using ultrafast laser radiation, with minimal substrate damage. Therefore, commercially available metallic mirrors (silver, aluminum, and gold) with a protective dielectric coating were irradiated with single-pulsed ultrafast laser radiation ($\tau_H = 40$ fs, $\lambda = 800$ nm). The obtained ablation structures (Fig. 1) were analyzed with respect to the ablation thresholds of the distinct included layers, and the used fluence was normalized to the ablation threshold H_{thr} for selective ablation of the dielectric coating. At fluences of 1.5 H_{thr}, the dielectric coating is partially ablated for the silver mirror (Fig. 1 a). In contrast, for the aluminum mirror, the entire multilayer system is removed at the center of the ablation structure at 1.5 H_{thr} (Fig. 1 b). On the other hand, only the dielectric coating is ablated from the gold layer at 1.5 H_{thr} (Fig. 1 c). To gain insights into the different ablation mechanisms that generate the three distinct ablation structures, the ablation processes were investigated using ultrafast metrology [1–4], and possible explanations were derived from the time-resolved dynamics.

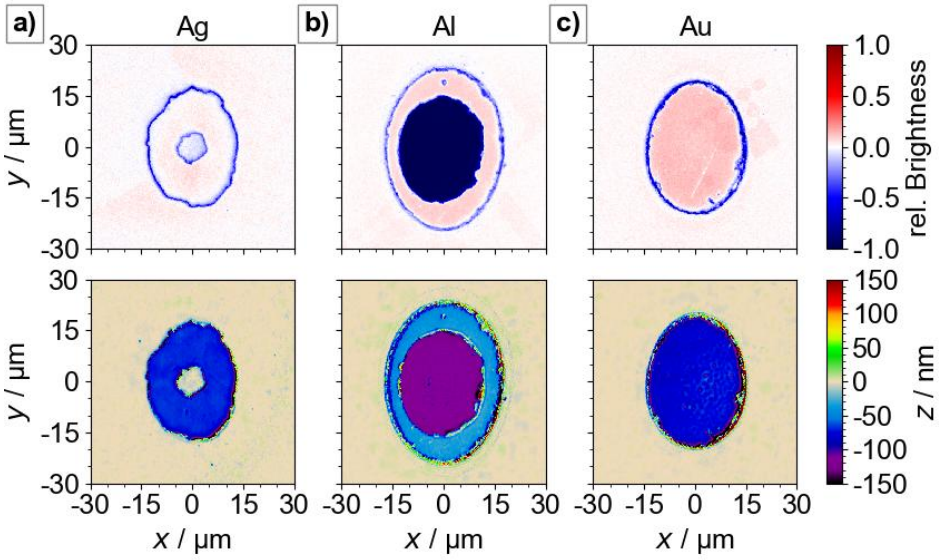


Figure. 1: Experimentally determined normalized relative brightness (top row) and topography (bottom row) of the ablation structures upon irradiation of commercially available a) silver, b) aluminum and c) gold mirrors with single-pulsed ultrafast laser radiation (pulse duration $\tau_H = 40$ fs, wavelength $\lambda_{Pump} = 800$ nm). The applied fluence is normalized to 1.5 times the threshold fluence of ablating the dielectric coating $H_0 = 1.5\ H_{thr}$ (Ag: $H_{thr} = 0{,}39$ J/cm², Al: $H_{thr} = 0{,}24$ J/cm, and Au: $H_{thr} = 0{,}37$ J/cm²).

Acknowledgement
The authors gratefully thank the Federal Ministry for Economic Affairs and Energy (BMWE) and the Industrial Collective Research (IGF) for funding the project SelektLas no. 01IF24626N.

References
1. T. Pflug, J. Pablo-Navarro, M.S. Anwar, M. Olbrich, C. Magén, M.R. Ibarra, K. Potzger, J. Faßbender, J. Lindner, A. Horn, R. Bali, Adv. Funct. Mater. **34**, 2311951 (2023), DOI:10.1002/adfm.202311951
2. T. Pflug, P. Cejpek, M. Olbrich, C. Wüstefeld, M. Ernstberger, M. Motylenko, D. Rafaja, A. Horn, Opt. Laser Technol. **172**, 110540 (2024), DOI:10.1016/j.optlastec.2023.110540
3. T. Pflug, M. Olbrich, H. Loheit, A. Horn, Appl. Phys. A **130**, 632 (2024), DOI:10.1007/s00339-024-07797-w
4. M. Olbrich, T. Pflug, A. Engel, A.F. Lasagni, A. Horn, Meas. Sci. Technol. (2026), DOI:10.1088/1361-6501/ae6679

Determining the influence of a protective dielectric coating on the ablation of metallic mirrors

Markus Olbrich[1,2], Vincent Rupf[1], Andy Engel[1], Robert Schmidt[3], Jens Bliedtner[3], Andrés Lasagni[2,4], and Alexander Horn[1]

[1]Laserinstitut Hochschule Mittweida, Technikumplatz 17, 09648 Mittweida

[2]Institut für Fertigungstechnik, TU Dresden, George-Bähr-Str. 3c, 01069 Dresden

[3]Ernst-Abbe-Hochschule Jena, Carl-Zeiss-Promenade 2, 07745 Jena

[4]Fraunhofer-Institut für Werkstoff- und Strahltechnik IWS, Winterbergstr. 28, 01277 Dresden

The selective removal of multilayer coatings from optical components, here commercially available metallic gold mirrors, is studied using single-pulsed ultrafast laser radiation ($\tau_H = 40$ fs, $\lambda = 800$ nm). Thereby, the topography of obtained ablation structures (Fig. 1 a), and thus the ablation threshold for ablating the distinct layers, differ completely from each other whether a dielectric coating is included or not. To explain the different ablation mechanisms in the presence of a dielectric coating and in its absence, the ablation process is theoretically studied using two-temperature hydrodynamics modeling [1] (Fig. 1 b) and experimentally using ultrafast metrology [2, 3]. As a result, the dielectric coating is ablated due to the emission of the shock- and rarefaction waves within the gold layer at fluences below the ablation threshold of the gold layer. On the other hand, the gentle and strong ablation thresholds for the gold layer are higher in the presence of the dielectric coating compared to its absence, being explained by a combination of the different propagation of the shock- and rarefaction waves compared to the case without a dielectric coating and the deceleration of the ablation plume by the dielectric coating.

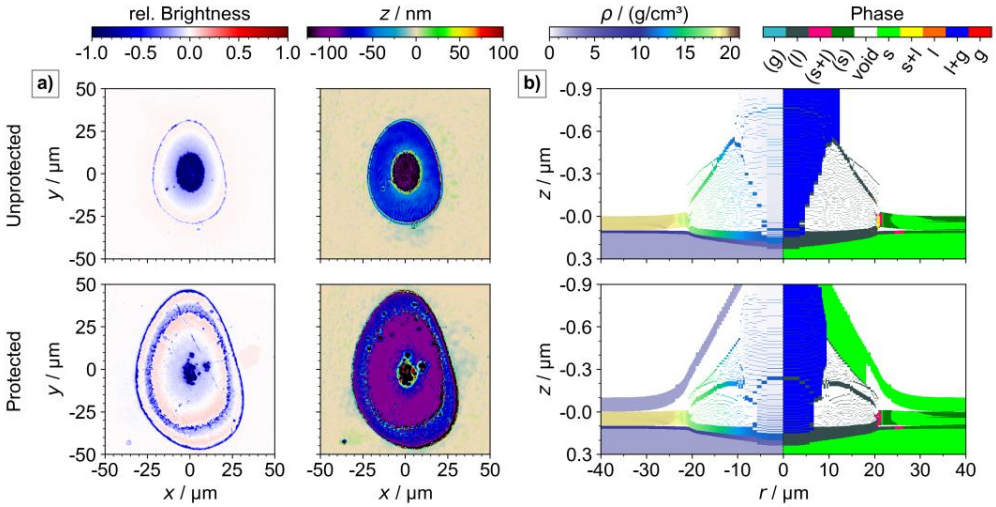


Figure 1: a) Measured white light micrograph (left col.) and topography (right col.) of the ablation structures upon irradiation of two gold mirrors with single-pulsed ultrafast laser radiation (τ_H = 40 fs, λ = 800 nm) and b) simulated ablation at t = 600 ps using the two-temperature model in combination with hydrodynamics (TTM-HD). The applied fluence is normalized to 4.0 times the ablation threshold H_{thr} of the gold layer (unprotected: H_{thr} = 0.65 J/cm² (top row), protected: H_{thr} = 1.05 J/cm² (bottom row)).

Acknowledgement

This research was funded by the German Federal Ministry for Economic Affairs and Energy (BMWE) within the Promotion of Joint Industrial Research Program (IGF) due to a decision of the German Bundestag. It was part of the research project 01IF24626N by the Association for Research in Precision Mechanics, Optics and Medical Technology (F.O.M.) under the auspices of the DLR Projektträger (DLR-PT).

References

1. M. Olbrich, T. Pflug, C. Wüstefeld, M. Motylenko, S. Sandfeld, D. Rafaja, A. Horn, Opt Lasers Eng **129**, 106067 (2020), DOI:10.1016/j.optlaseng.2020.106067
2. T. Pflug, J. Pablo-Navarro, M.S. Anwar, M. Olbrich, C. Magén, M.R. Ibarra, K. Potzger, J. Faßbender, J. Lindner, A. Horn, R. Bali, Adv. Funct. Mater. **34**, 2311951 (2023), DOI:10.1002/adfm.202311951
3. M. Olbrich, T. Pflug, A. Engel, A.F. Lasagni, A. Horn, Meas. Sci. Technol. **37**, 195202 (2026), DOI:10.1088/1361-6501/ae6679

LASER 2000
Experts in Photonics

Enabling Diverse Laser Applications with Customized Photonic Solutions

Abstract by Vincent Prévost, Laser 2000 GmbH

Laser systems are used in an exceptionally wide range of applications – from materials processing and micro structuring to life sciences, spectroscopy, metrology, and quantum technologies. Each of these fields places distinct and often conflicting demands on the laser sources and optical components in terms of wavelength coverage, output power and stability, pulse duration, coherence, modulation capability and long term reliability.

This talk presents an application driven overview of how current photonic technologies address these challenges, showcasing selected laser sources, optical components, and system solutions available through the Laser 2000 product portfolio and its international partners.

Special emphasis is placed on the integration of laser sources with beam delivery and diagnostics as well as laser safety products to form robust and scalable solutions. Beyond individual products, the presentation highlights how close collaboration between users, manufacturers, and distributors helps translate rapidly evolving laser technologies into real world applications.

Contact:

Vincent Prévost / Technical Sales & Photonics Advisor

Laser 2000 GmbH
Argelsrieder Feld 22
82234 Wessling / Germany

Mobil +33 6 64 48 45 03
E-Mail v.prevost@laser2000.fr
LinkedIn Vincent Prévost | LinkedIn

Overcoming Rayleigh – Characterization of ring-shaped laser beams in a systematic way

Author: Kris Rudolph, PRIMES GmbH
Address: Max-Planck-Str. 2
64319 Pfungstadt
Tel.: +49 6157 9878 115
Mail: k.rudolph@primes.de

Keywords: Beam shaping, Ring Beams, Beam Profiling, Caustic Analysis

Abstract:

The ISO 11146 standard provides a framework for characterizing common single- or multimode laser beams. Key parameters include the beam propagation ratio M², the beam width according to second-order moments d_σ, and the Rayleigh length z_R. However, beam shaping technologies are increasingly being adopted in materials processing. The most common examples are ring-shaped beams, which introduce distinct characteristics that are challenging to describe meaningfully using classical methods. This is particularly evident for mixed beams consisting of a central spot and a surrounding ring.

This work demonstrates the shortcomings of characterizing ring-shaped beams according to ISO 11146 and introduces a set of parameters designed to describe these beams in an appropriate and application-oriented manner. These parameters aim to provide quantities equivalent to classical parameters, thereby reducing the effort required to translate measurements into real-world processes. Using exemplary measurements of various ring beam profiles, a comparison between the proposed and the classical parameters is conducted.

Furthermore, different measurement principles employed by established beam profilers are compared to provide an insight into the interaction of the time-dependent behavior of the laser and its power distribution and the measurement principle. Finally, an optimized approach for measuring structured beam caustics is presented.

Focusing ultrashort UV pulses with industrial objectives: Onset and impact of spatiotemporal effects

Dario Mekle,[a,c] Roman A. Surma,[a] Julian Hellstern,[b] Martin Wimmer,[a]
Stefan Nolte,[c,d] and Daniel Flamm[a]

[a]TRUMPF Laser- und Systemtechnik SE, 71254 Ditzingen, Germany
[b]TRUMPF Laser SE, 78713 Schramberg, Germany
[c]Friedrich Schiller University Jena, Institute of Applied Physics, Abbe Center of Photonics, 07745 Jena, Germany
[d]Fraunhofer Institute for Applied Optics and Precision Engineering IOF Jena, Center of Excellence in Photonics, 07745 Jena, Germany

ABSTRACT

This study analyzes the spatiotemporal behavior of ultrashort UV pulses focused by common industrial focusing objectives at 343 nm. A combination of pupil-resolved ray tracing and wave-optical propagation is used to reconstruct the focal space–time intensity distribution, including pupil-dependent space–time couplings and Kerr lensing. We investigate the focus quality as a function of pulse duration from the picosecond to the sub-100 fs regime for representative objectives used in laser micromachining. The analysis identifies the pulse-duration range in which chromatic dispersion, wavelength-dependent aberrations and nonlinear lensing become critical for focal pulse duration, Strehl ratio and peak intensity.

Keywords: Ultrafast optics, optical design, laser materials processing, micromachining, structured light, light-matter-interaction

Further author information:
E-Mail: dario.mekle@trumpf.com.

Dynamic beam shaping with a multicore-fiber-based, high-power, femtosecond CPA laser system

Arno Klenke[1,2,3,4*], Chandroth P. Jisha[1], Felix Wanitschke[1,2,3], Alessandro Alberucci[1], Mehran Bahri[1], Yahia Khalil[1], Cesar Jauregui[1,4], Johannes Nold[4], Stefan Kuhn[4], Nicoletta Haarlammert[4], Thomas Schreiber[4], Stefan Nolte[1,4] and Jens Limpert[1,2,3,4]

[1]Friedrich Schiller University Jena, Institute of Applied Physics, Abbe Center of Photonics, Albert-Einstein-Straße 15, 07745 Jena, Germany
[2]Helmholtz-Institute Jena, Fröbelstieg 3, 07743 Jena, Germany
[3]GSI Helmholtzzentrum für Schwerionenforschung, Planckstraße 1, 64291 Darmstadt, Germany
[4]Fraunhofer Institute for Applied Optics and Precision Engineering, Albert-Einstein-Straße 7, 07745 Jena, Germany
Author e-mail address: a.klenke@hi-jena.gsi.de

Controlling the phases of a coherently combined laser beam array enables dynamic beam-shaping for subsequent applications. One use case is that of fast beam pattern switching in the field of materials processing, e.g. to avoid limitations due to heat accumulation in the material [1]. Multicore fibers (MCFs) allow for massively parallelized amplification. In this context, both theoretical and experimental [2] results have highlighted the impressive scaling potential of both the average power and pulse energy, enabling access to multi-kW average powers and femtosecond pulses with energies in the multi-mJ range.
In this experiment the radiation from a femtosecond frontend is split up into a beam array before being amplified in two 49-core Ytterbium-doped fibers, recompressed and, finally, recombined. A MEMS phase actuator array in front of the first multicore fiber enables phase control of individual beams with up to kHz frequencies. Using a photodiode and stabilization electronics, the position of the phase actuators can be optimized to maximize the combined power in the central lobe of the beam pattern using the SPGD algorithm. Adding additional phase patterns allows manipulating the beam image, for example steering the central lobe or generating optical angular momentum (OAM) beams.

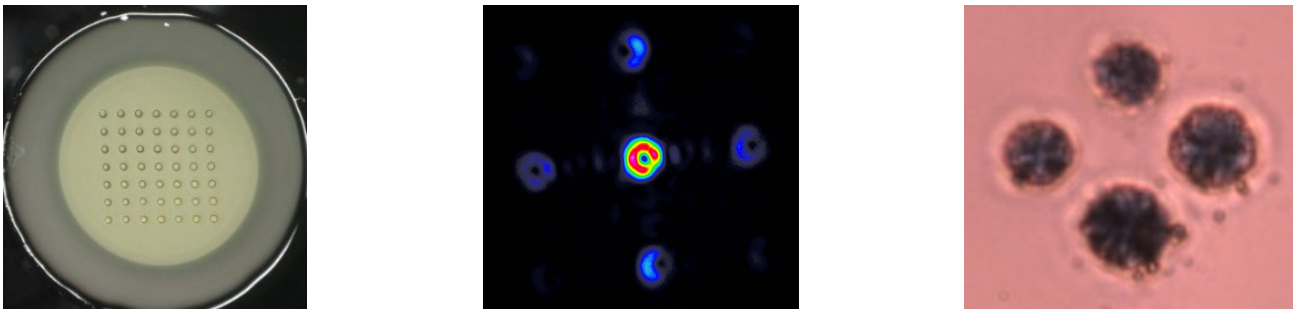


Fig. 1. Left: Microscope image of the fiber end facet, Center: Shaped optical angular momentum beam, Right: Ablation experiment where a two-lobe beam was dynamically switched between two orientations

We have achieved a total average power of 150 W behind the compressor with a pulse repetition rate of 148 kHz. With this laser system we could demonstrate first materials processing results, such as structured ablation of a glass substrate with fast beam switching.

1. F. Bauer, A. Michalowski, T. Kiedrowski, and S. Nolte, "Heat accumulation in ultra-short pulsed scanning laser ablation of metals," Opt. Express **23**, 1035-1043 (2015)
2. 1. A. Klenke, C. Jauregui, M. Bahri, J. Nold, S. Kuhn, N. Haarlammert, T. Schreiber, and J. Limpert, "High-power ytterbium-doped multicore fibers," Opt. Fiber Technol. **96**, 104471 (2026).

Low-loss femtosecond-written waveguides for co-packaged optics

Namig Alasgarzade[1], Alessandro Alberucci[1], Martin Letz[2], Degenhart Hochfilzer[2], Jens Ulrich Thomas[2], and Stefan Nolte[1,3]
[1]Friedrich Schiller University Jena, Institute of Applied Physics, Abbe Center of Photonics, Albert-Einstein-Straße 15, 07745 Jena, Germany
[2]SCHOTT AG, Hattenbergstraße 10, 55122 Mainz, Germany
[3]Fraunhofer Institute for Applied Optics and Precision Engineering, Albert-Einstein-Straße 7, 07745 Jena, Germany
Author e-mail address: stefan.nolte@uni-jena.de

Optical waveguides play a central role in photonic applications, permitting the confinement of light in narrow regions of space and its re-routing along complex spatial trajectories. Nonlinear optics can be exploited to realize complicated networks of waveguides in the bulk of arbitrarily shaped glass samples [1]. When ultrashort optical pulses are tightly focused inside a glass, a local change in the refractive index can be permanently written, once the intensity overcomes a material-dependent threshold. In several glasses a positive change in the refractive index can be written. When the laser parameters are properly chosen, the inhomogeneities induced in the glass can induce total internal reflection and, thus, waveguiding. The great advantage is that these laser-written waveguides, once aberrations are properly compensated for, can be placed anywhere in the sample.
The unique 3D properties of fs-written waveguides find direct applications in microelectronics: these waveguides can be used as very versatile connectors between optical fibers and photonic chips [2,3]. Beyond microelectronics, other potential applications are the realization of integrated circuits for sensing and medical diagnostics over wafer level.
In this contribution we analyze the performances of fs-written waveguides written in three different multicomponent glasses -AF32, AF35G and D263T- selected from the Schott catalogue. In fact, fs-written waveguides in borosilicate glasses have been shown to perform excellently. Industrially speaking, we chose glasses that can be produced in wafers or panels, thus ensuring large scaling in the manufacturing process. For all the glasses, we tested all the main writing parameters to find the optimal writing configuration. In doing that, losses below 0.3 dB/cm are demonstrated in all the three glasses, therefore showing their potentiality in future applications based upon integrated optoelectronics.

1. A. Szameit and S. Nolte, "Discrete optics in femtosecond-laser-written photonics structures," J. Phys. B **43**, 163001 (2010)
2. G. Djogo, J. Li, S. Ho, M. Haque, E. Ertorer, J. Liu, X. Song, J. Suo, and P. R. Herman, “Femtosecond laser additive and subtractive micro-processing: enabling a high-channel-density silica interposer for multi-core fibre to silicon-photonic packaging,” Int. J. Extreme Manuf. **1,** 045002 (2019).
3. T.T. Fernandez, S. Gross, K. Privat, B. Johnston, and M. Withford, “Designer glasses—future of photonic device platforms”, Adv. Funct. Mater. ***32***, 2103103 (2022).

The Femtosecond Laser as a Versatile Tool for Fabricating All-Glass Atomic Vapor Cells for Quantum Applications

A novel method for fabricating all-glass atomic vapor cells is presented. Glass substrates of standard optical quality are structured using femtosecond (fs) laser ablation and mechanical machining. The structured substrates are then hermetically bonded via optical contact bonding under vacuum or buffer gas atmosphere. Subsequent fs-laser welding reinforcement significantly improves the tensile strength and thermo-mechanical resilience of the joint, thereby ensuring long-term vacuum tightness. Cesium or rubidium is released from an alkali metal getter pellet inside the cell by fs-laser ablation. If necessary, excess reaction byproducts of the getter pellet that obstruct the internal windows of the cell are removed in a final step by cleaning via fs-laser backside ablation. The entire fabrication process avoids elevated temperatures, enabling future integration of sensitive internal coatings (e.g., paraffin or silane films) to enhance spin coherence for quantum sensing applications. Absorption spectroscopy confirms hermetic sealing and excellent long-term stability over 10 months, with no detectable gas ingress or alkali metal loss.

High-Power Diode Laser Pump Modules for Solid State Laser-Driven Fusion Reactors

E. Werner[1)], M. Zorn[2)], R. Hülsewede[2)], M. Salge[1)], J. Meusel[1)], M. Stier[1)], M. Schröder[1)], T. Kaaden[1)]

[1)]Jenoptik Optical Systems GmbH, Göschwitzer Straße 25, 07745 Jena

[2)]Jenoptik Optical Systems GmbH, Max-Planck-Straße 2, 12489 Berlin

ekkehard.werner@jenoptik.com, Tel. 03641-654319

The development of an inertial confinement fusion power plant based on solid state lasers relies heavily on the availability of custom-designed, high-efficiency, and low-cost diode laser pump modules. Currently, commercial pump sources do not meet the required performance and cost targets, and the demand for high-power diode laser bars for a single plant would exceed the present global annual production capacity. Therefore, significant technological advancements are necessary to overcome these limitations.

Jenoptik as part of the government-funded DioHELIOS project, a collaboration between leading German laser manufacturers and research institutes, addresses key challenges along the entire value chain of diode laser pump modules. Jenoptik's contributions in Jena and Berlin focus on:

- Designing optimized diode laser bars with improved efficiency and geometry (size, thickness, fill factor) at wavelengths of 880 nm and 940 nm with optional wavelength stabilization
- Adapting assembly technology for diode laser bars to accommodate resonator lengths of 4 mm for enabling output powers of 1 kW (short pulse mode) per bar and reducing bar pitch to increase power density of the stacks
- Optimizing diode stack design to achieve effective scalability of stacks for compact pump modules with high laser beam density
- Developing and refining diode laser technology, including bar-integrated wavelength stabilization and multi-junction emitters – both required for increasing pumping efficiency.

The DioHELIOS project consortium aims to deliver a scalable concept for high-energy pump sources and validate it with laboratory demonstrators capable of delivering 1 MW peak power on a custom-developed measurement bench. This work lays the foundation for economically viable, high-performance pump modules essential for future solid-state laser-driven fusion reactors.

Tailored nanostructured AR coatings for high-intensity laser systems

E. Fürch[1,2], A. Bingel[1], F. Rickelt[1], U. Schulz[1], C. Mühlig[1], T. Herffurth[1], A. Ribeaud[1], E. Upol Biswas[1,2], A. Szeghalmi[1], S. Schröder[1], A. Tünnermann[1,2]

[1] Fraunhofer Institute for Applied Optics and Precision Engineering IOF, Germany
[2] Institute of Applied Physics, Friedrich Schiller University Jena, Germany

Future high-energy laser systems, such as those used in laser inertial fusion, require optical components with very high transmission, low absorption, and high stability under intense laser irradiation. Although conventional antireflective (AR) coatings have been well studied and show very good performance, they can still reach their limits in high-energy laser applications due to absorption, thermal stress, and local electric field enhancement. Nanostructured AR coatings offer a promising alternative, as they can be fabricated entirely from wide-bandgap materials such as SiO_2, which naturally exhibit very low absorption and are therefore well suited for high laser intensities.

This work presents nanostructured moth-eye AR coatings on fused silica fabricated using the AR-plas2 process developed at Fraunhofer IOF. The process is based on an Ar/O_2 plasma etching step of an organic thin film with the APSpro (Advanced Plasma Source), which is integrated into a commercially vacuum box coater from Bühler Leybold Optics. The plasma-structured organic thin films are coated with SiO_2, after which the organic template is removed. This results in nanostructured SiO_2 layers with tunable effective refractive indices down to 1.05. These layers can be described as single $\lambda/4$ coatings with low effective index and provide antireflective properties through interference effects. The coating design can be adapted to wavelengths relevant for high-power laser systems from UV to NIR, e.g. 351 nm, 527 nm, and 1053 nm as they are used in laser inertial fusion reactors.

The samples investigated in this work are optimized for a laser wavelength of 1064 nm. Optical and energetic characterization is performed with emphasis on minimizing absorption and scattering losses. Using laser-induced deflection measurements, absorption values as low as 2 ppm have already been achieved at both 355 nm and 1064 nm. A central focus of this study is the comparison between nanostructured moth-eye coatings, conventional unstructured ion-beam-sputtered (IBS) coatings, and conformal nanoporous SiO_2 layers deposited by atomic layer deposition (ALD).

Entwicklung Cr-(VI)-freie schwarze Nickelschichten mit angepassten Eigenschaften für die Optikbranche- und Laserindustrie

Kameras und optisch arbeitende Messverfahren haben insbesondere mit der Entwicklung von leistungsfähigen elektrooptischen Mess- und Aufnahmechips eine große Verbreitung gefunden. Um eine gute Abbildungsqualität zu erreichen bzw. um die Genauigkeit der Messergebnisse zu erhöhen, müssen die Gehäusebauteile von optischen Geräten zur Vermeidung von Streulicht, auch Falschlicht genannt, innen mattschwarz beschichtet werden. Innerhalb der nasschemischen Metallisierungsverfahren existiert eine Methode um im Vergleich zum Schwarzverchromen REACH-konforme, korrosionsbeständige und mechanisch widerstandsfähige schwarze Metallschichten zu erzeugen, welche im Zuge eines drohenden Chrom-(VI)-Verbotes für industrielle Beschichtungsprozesse eine Alternative bieten. Die Rede ist von stromlos abgeschiedenem Chemisch Nickel. Die Schwarzfärbung der Nickelschichten erfolgte im Rahmen eines von INNOVENT e.V. und weiteren Industriepartnern durchgeführten Forschungsprojektes mit dem Ziel optische Eigenschaften (z.B. Reflexion und Absorption) für den Einsatz innerhalb der Optik-, Lasertechnik- und Luft- und Raumfahrtbranche anzupassen. Dafür wurden unterschiedliche Methoden der Schwarzfärbung für chemisch Nickel - von kommerziell erhältlichen, literaturbekannten bis hin zu eigen synthetisierten Färbelösungen – untersucht, zusammengefasst und miteinander verglichen. Daneben stellte sich unter anderem die Frage welche Möglichkeiten der Vor- und Nachbehandlung von Substraten es gibt um die optischen Eigenschaften gezielt zu beeinflussen? Neben der Applikation von SiOx-Schichten durch Plasmabehandlung und Beflammungstechnik und der Anwendung von hauseigen entwickelten Sol-Gel-Beschichtungen wurden Sandstahlverfahren als Vorbehandlungsschritt eingesetzt um optische Eigenschaften zu verändern und in einigen Fällen die Reflexion zu mindern. Um die Mechanismen die zur Schwärzung des Chemisch Nickels beitragen besser zu verstehen, fanden Untersuchung der Oberflächenbeschaffenheit mit Hilfe von Konfokal- und Rasterelektronenmikroskopie statt, sowie die Analyse der chemischen Zusammensetzung mittels Röntgenfluoreszenzspektroskopie (RFA), Energiedispersive Röntgenspektroskopie (EDX), Röntgenphotoelektronenspektroskopie (XPS) und weiterer Verfahren statt.

Direct Ultrashort Pulsed Laser Welding of Zerodur to Stainless Steel

Münch, M.[1]; Sohr, D[1]; Margraf, J.[1,2]; Nolte, S.[1,2]
[1]Friedrich Schiller University Jena, Institute of Applied Physics, Abbe Center of Photonics, Jena, Germany
[2]Fraunhofer Institute for Applied Optics and Precision Engineering IOF, Jena, Germany

Applications such as electronic packaging, precision optics, sensor technology, and medical devices frequently require joining dissimilar materials, including at least one optical component, while ensuring water- and gas-tight sealing. Achieving such joints with conventional processes remains challenging, as they typically induce thermal stress and large heat-affected zones that degrade both optical quality and mechanical performance. Ultrashort pulsed lasers enable highly localized energy deposition and a small heat-affected zone, helping to minimize thermally induced stress in the joining area. In this work, gastight joints between Zerodur and stainless steel grades 1.4201 and 1.4404 were produced using ultrashort pulsed laser welding, achieving helium leak rates down to 10^{-9} mbar·L/s. Mechanical performance was evaluated by tensile testing. The results demonstrate the feasibility of gastight glass–metal joining by ultrashort pulsed laser processing and indicate further optimization potential.

Opportunities and Challenges in Glass Processing with Ultrashort Pulse Lasers

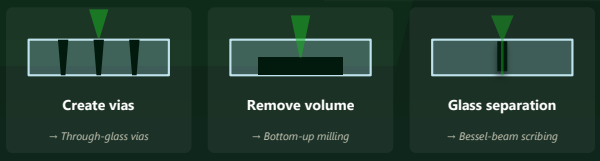
EKSPLA TOPAG

Deividas Andriukaitis[1], Christian Bischoff[2]
[1] Ekspla, Savanoriu ave. 237, LT-02300 Vilnius, Lithuania · d.andriukaitis@ekspla.com
[2] Topag, Nieder-Ramstädter Str. 247, 64285 Darmstadt, Germany · bischoff@topag.de

JLT15, XV Jenaer Lasertagung

Processing Glass Challenges

Glass is transparent and brittle, for precise and high-quality processing traditional mechanical methods fall short. Femtosecond lasers can process glass without significant defect formation. We address **three applications:**



Create vias	Remove volume	Glass separation
→ Through-glass vias	→ Bottom-up milling	→ Bessel-beam scribing

Process Challenges

Repeatability | Throughput | Process speed and quality

FemtoLux - Industrial Femtosecond Lasers



Industrial femtosecond laser **FemtoLux** designed from the get-go for maximum **reliability**, seamless integration and non-stop 24/7/365 **zero maintenance** operation.

Wide range of **options** enable to tailor this ultrafast laser for desired material processing tasks.

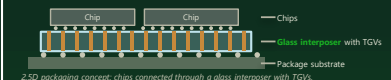
Wavelength	1030/515/343 nm	Power stability	< 0.5 % RMS over 100 hours
Average power	Up to 50 W	Energy stability	< 1 % StDev
Pulse duration	Down to 350 fs	PoD	20 ns jitter, down to single-shot
Beam quality	Typically M^2 < 1.1, ellipticity >0.9	Cooling	DRC (no maintenance) / Water



Through-glass vias

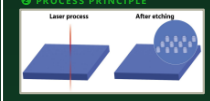
❶ APPLICATION NEED

Glass interposers for 2.5D packaging need dense via arrays: **with high yield and repeatability**



2.5D packaging concept: chips connected through a glass interposer with TGVs.

❷ PROCESS PRINCIPLE

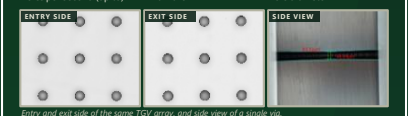


Laser process
Ultrashort pulses modify the glass along each via path.

Selective etching
The modified glass etches away much faster — the via opens with vertical walls [1].

❸ DEMONSTRATED RESULT

5000/s holes per second (up to) | **Vertical** via walls | **Tunable** hole diameter



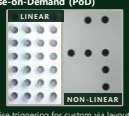
Entry and exit side of the same TGV array, and side view of a single via.

Challenge - TGV repeatability – defective TGV requirements:

2024–2025 ~100 ppm → 2025–2026 ~10–20 ppm → > 2026 ~1–5 ppm

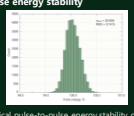
5 ppm = 5 defective TGVs in 1 000 000 TGVs.

Pulse-on-Demand (PoD)



Precise triggering for custom via layouts: in non-linear matrices speed and repetition rate vary.

Pulse energy stability



Typical pulse-to-pulse energy stability of FemtoLux 30 at 200 kHz.

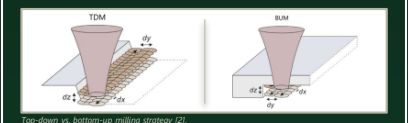
Bottom-up milling

❶ APPLICATION NEED

Remove large glass volumes – trenches, holes, pockets in thick glass: **with high throughput**

❷ PROCESS PRINCIPLE

Top-down milling (TDM) removes glass layer by layer — ideal for fine features, but debris limits deep geometries. In **bottom-up milling (BUM)** the beam is focused at the rear surface: debris leaves through the backside and long **MHz+GHz bursts** remove glass in larger chips [2].

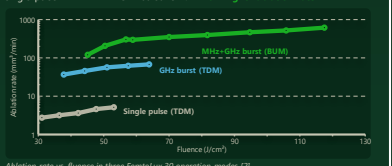


Top-down vs. bottom-up milling strategy [2].

❸ DEMONSTRATED RESULT

5.17 → 619.5 mm³/min

single-pulse TDM → MHz+GHz burst BUM: **~120× higher ablation rate**

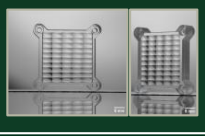


Ablation rate vs. fluence in three FemtoLux 30 operation modes [2].

Speed vs quality - trade-off

Sa 191 nm single-pulse TDM → **Sa 4.3 µm** MHz+GHz burst BUM

Switch modes: single pulses for fine features, bursts for fast rough machining.



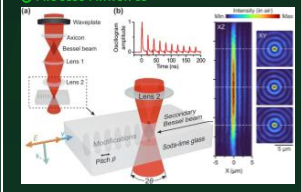
Demonstration:
fused-silica micro-lens array
25 × 25 mm², 50 lenses (R = 5 mm). Base cut with burst BUM in **13 min** (180 mm³/min); lenses with TDM (**Sa 0.5 µm**); and CO_2-laser polishing to **23 nm** [2].

Bessel-beam scribing

❶ APPLICATION NEED

Separate glass thick glass along defined paths with clean edges: **with high process speed and quality**

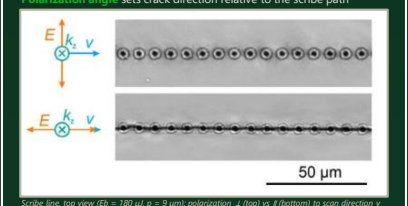
❷ PROCESS PRINCIPLE



An **axicon** forms a Bessel beam: one elongated focus modifies the full thickness in a single pass.
A **separate cleaving step** (mechanical or CO_2-laser-assisted) completes separation

❸ DEMONSTRATED RESULT

Polarization angle sets crack direction relative to the scribe path



Scribe line, top view (Eb = 180 µJ, p = 9 µm): polarization ⊥ (top) vs ∥ (bottom) to scan direction v [3].

Ra < 1 µm | **140 mm/s** | **180 µJ**

PROCESS CONDITIONS

Burst	10 pulses · 50 MHz intra-burst
Repetition rate	20 kHz
Optics	5° axicon Bessel beam
Glass	1 mm soda-lime (up to 4.8 mm)

Summary

FemtoLux — one versatile source for glass processing

Single pulses, MHz, GHz and MHz + GHz bursts and Pulse-on-Demand triggering let one industrial laser address very different glass applications — from precise via formation to high-throughput milling and clean separation.

THROUGH-GLASS VIAS
5000/s
holes second (up to) by selective laser etching

BOTTOM-UP MILLING
619.5 mm³/min
glass removal rate, ~120× single-pulse TDM

BESSEL-BEAM SCRIBING
4.8 mm
thick soda-lime glass scribed; Ra < 1 µm sidewalls

Explore more applications

Scan to discover more FemtoLux applications
Material Processing section on our webpage.

Our application lab is open for tests
Bring your samples — we will test them with FemtoLux.
Contact: **d.andriukaitis@ekspla.com**

REFERENCES AND
[1] https://www.rena.com/en/products/glass-sapphire/through-glass-vias-tgv
[2] Ekspla application note, "Hybrid Laser Processing of Micro-Lens Arrays Using the FemtoLux 30", rev. 250429 (2025).
[3] J. Dudutis, A. Kondratas, P. Gečys, ACS Photonics 12(7), 3706–3716 (2025).
TGV results courtesy of Workshop of Photonics.

DISTRIBUTOR IN GERMANY

TOPAG

TOPAG Lasertechnik GmbH
Nieder-Ramstädter Str. 247, 64285 Darmstadt
www.topag.de · info@topag.de

Plug-and-Play kHz Laser Control System for Advanced Fluorescence Microscopy

Josephine Meitzner, Sascha Klötzer, Richard Börner

Laserinstitut Hochschule Mittweida, University of Applied Sciences Mittweida, Germany

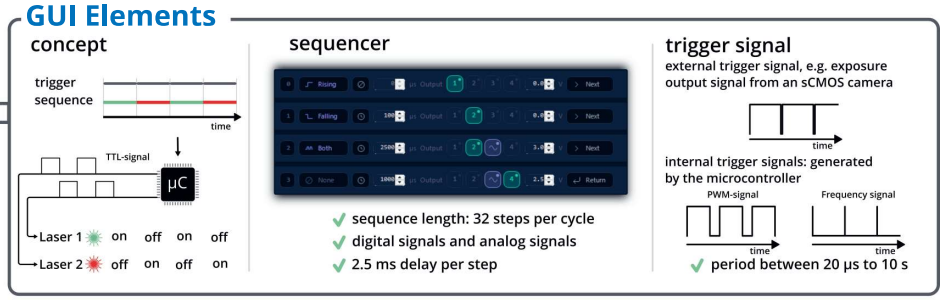
Laser-Output

kHz Laser-Controller

Introduction

Single-molecule microscopy utilizing alternating laser excitation (ALEX) is an established method for the characterization of biomolecules [1,2]. However, existing laser control systems are often costly and OEM-specific, limiting flexibility in customized microscopy environments. To overcome these limitations, we developed an independent, user-friendly laser control approach based on a microcontroller architecture capable of managing up to four individual laser sources. The system is specifically designed for advanced fluorescence microscopy, allowing users to implement preconfigured as well as fully customizable triggering schemes via an intuitive graphical user interface (GUI). This enables complex illumination modes such as ALEX/sALEX for total internal reflection fluorescence (TIRF) and confocal fluorescence microscopy assays [3,4].

GUI Elements

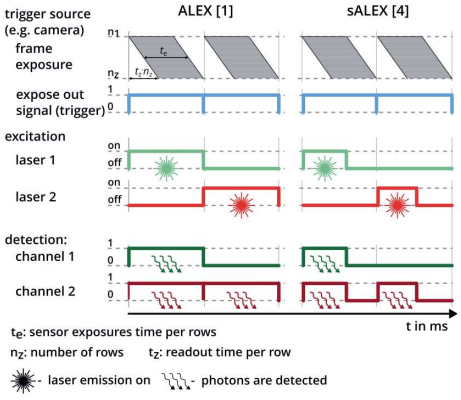


Hardware

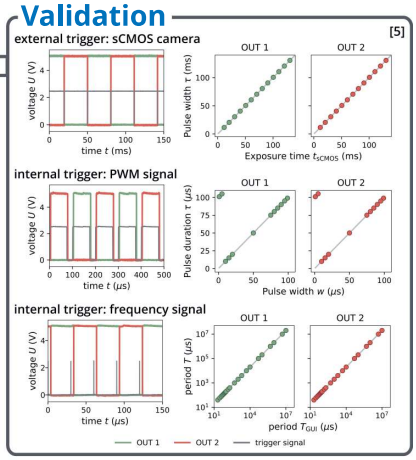


- 8-bit microcontroller
- 4 digital outputs → 3 configurable as analog outputs (0 - 5 V)
- 2 digital inputs
- 1 analog input (0 - 20 V)

Excitation Schemes



Validation



Key Features

- **50 kHz** maximum repetition rate
- **20 µs - 10 s** programmable timing range
- Predefined excitation schemes: **ALEX/sALEX for 2 - 4 lasers**
- Custom sequence editor: **up to 32 steps**
- **Frequency & PWM signal generation**

Outlook

Bluetooth, mobile app, MHz, user experience,...

Acknowledgement

JM and RB received funding from SMWK-Forschungsförderung "Innovations-Cluster 2023". Furthermore JM thanks for the financial support from the "Promotionsstipendium zur Förderung von Frauen in Wissenschaft und Forschung an der Hochschule Mittweida". We would also like to thank University of Applied Sciences Mittweida and the Laserinstitut Hochschule Mittweida for their support.

References

[1] A. Kapanidis, et al., PNAS 2004, 101, 8936-8941
[2] R. Börner, et al., PLOS ONE 2018, 13
[3] A. Yang, et al., Open Conference Proceedings 2022, 2, 39–43
[4] J. Hohlbein, et al., Chem. Soc. Rev. 2014, 43, 1156–1171
[5] J. Meitzner, master thesis, Hochschule Mittweida 2026 (under embargo)

Laserinstitut Hochschule Mittweida
Technikumplatz 17, 09648 Mittweida
Josephine Meitzner, M.Sc. | meitzner@hs-mittweida.de
Richard Börner, PhD | richard.boerner@hs-mittweida.de

www.laser.hs-mittweida.de

Börner-Lab

GitHub

CiS Forschungsinstitut für Mikrosensorik GmbH

Investigation of Laser Parameters for the Creation of Traces and Contact Pads on Aluminum Nitride Ceramics

F.-M. Deckert[1], C. Heinze[1], M. Kermann[1], I. Käpplinger[1], and T. Ortlepp[1]
[1] *CiS Forschungsinstitut für Mikrosensorik GmbH, Konrad-Zuse-Straße 14, 99099 Erfurt, Germany*
fdeckert@cismst.de

Motivation

The development of sensor and actuator units is closely linked with the development and design of suitable circuit boards. Due to variations in the layout of those microsystems an economical and adaptable process for the individual structuring of the circuit boards is needed [1]. Addressing these needs the laser ablation of aluminum nitride (AlN) was applied to create conductive traces and pads.

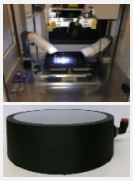
Methode

Investigation of laser parameters

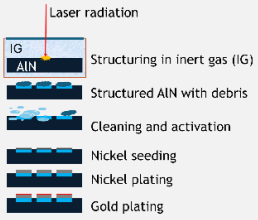
The laser ablation was carried out in the Rofin-Sinar 100D laser system at a wavelength λ of 1064 nm. An Alunit ceramic (CeramTec GmbH) was used as the substrate. The laser-radiation composed of h (Planck's constant) and the light frequency υ enables the thermal decomposition of the AlN substrate into Al and nitrogen (N_2) [2, 3]:

$$AlN + h\nu_{Laser} \rightarrow Al + \frac{1}{2} N_2 \quad (1)$$

Besides the laser parameters like pulse energy, focus depth, and more, the process is influences by the atmosphere. Therefore, a 3D printed cylindrical beaker with a laser protection glass on top and a hose connection at the outer wall was used to establish an inert gas atmosphere.



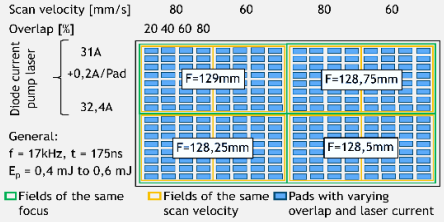
Top: Interior of Rofin laser
Bottom: Inert gas chamber



Process flow chart

Wet chemical processes

To facilitate electrodeposition, samples require cleaning following laser ablation. For this purpose the AK180 degreaser (Dr.-Ing. Max Schlötter GmbH & Co. KG) was used in an ultrasonic bath. Afterwards, the Al was seeded with Nickel (Ni) by a Ni-sulfate based strike solution at a pH of 7.5.
Subsequently, a Ni layer up to 12 µm was plated on top of the Ni seeding layer. The Ni was plated with the EN2310 electrolyte (Dr.-Ing. Max Schlötter GmbH & Co. KG). The next step was the deposition of a 30 nm to 50 nm Au layer by the usage of the Xenolyte Au CF2 (Atotech Deutschland GmbH & Co. KG).



Paradigmatic laser parameters

Results

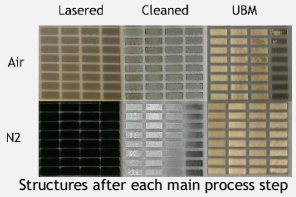
Laser ablation and plating

The investigation shows that the transformation depends primarily on the diode current of the pump laser, the overlap, and the atmosphere in the process chamber. The roughness of the structures is mainly related to the diode current and the overlap. Whereby an increasing current and decreasing overlap results in rougher structures. The advantage of the high roughness is the enhanced physical interconnection between the ceramic substrate and the deposited layers. This results in a high breaking force regarding bump and wire bonding (see table). On the other hand leads the roughness to a longer plating time to realize a dense and closed Ni layer without pores.

Results of adhesion testing

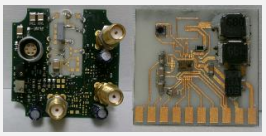
Method \ Parameter	Mean breaking force [g]	Required force [g]
Bump shear test Au Bumps	58	27
	66	
	64	
	60	
Wire pull test Wedge-Wedge-Al	19	9
	19	
	22	

Below the influence of the two different process atmospheres on the complete process are depicted as well as current applications for sensor prototyping.



Structures after each main process step

Charge sensitive preamplifier for photodiodes



Integrated digitally adjustable step-down converter to control one individual or a series of UV-LED(s)

Conclusion

This process flow shows one possibility for a fast and individual manufacturing of circuit boards for sensor prototyping.
One drawback is the thin Al layer whereby the connection of the Ni and AlN is weak. Therefore, further investigations are planned to increases the thickness of the Al layer and enhanced the connection of Ni-AlN interface
Future applications include the usage of these circuit boards in a cryogenic environment.

References

[1] A. Mukhopadhyay et al., "Laser-tuned surface wettability modification and incorporation of aluminum nitride (AlN)Ceramics in Thermal Management Devices", Advanced Functional Materials 34 (2024), 2313141.
[2] A.J. Antończak et al., "Direct selective metallization of AlN ceramics induced by laser radiation", Laser-based Micro- and Nanoprocessing VIII, Proc. of SPIE Vol. 8968 (2014), 896814.
[3] P.E. Kozioł et al., "Conductive aluminium line formation on aluminium nitride surface by infrared nanosecond laser", Applied Surface Science 287 (2013) 165-1

Kofinanziert von der Europäischen Union
Thüringer Aufbaubank Die Förderbank.
Ernst-Abbe-Hochschule Jena University of Applied Sciences

Energy-Efficient Laser Beam Hardening

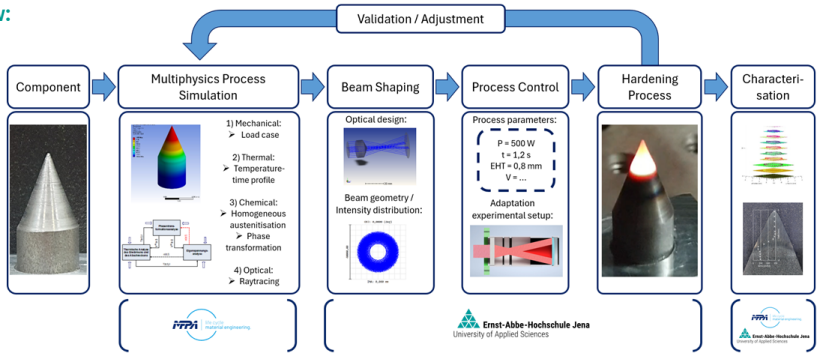
Michael Güpner[1], Lisa Tewes[1], Frank Rempt[1], Andreas Hopf[1], Jens Bliedtner[1], Lukas Werner[1], Robert Brunner[1], Andreas Diemar[2], Susanne Kleemann[2], Tom Lahmer[2]

[1]Ernst-Abbe-Hochschule Jena, Carl-Zeiss-Promenade 2, 07745 Jena
[2]Materialforschungs- und -prüfanstalt an der Bauhaus-Universität Weimar, Coudraystraße 9, 99423 Weimar

Laser beam hardening is already an established industrial process. In industrial practice, the process parameters are typically selected based on operator's extensive experience and empirical knowledge accumulated over many years. The beam geometries and intensity profiles employed are often linear or rectangular, with variable dimensions and a top-hat intensity distribution. For laser beam hardening, significant gains in process efficiency and improvements in hardening performance can be achieved by tailoring the beam geometry and intensity profile to the specific functional requirements and geometry of the component. Building on this, the "HardLight" research group is developing a simulation-based workflow for laser beam hardening that integrates the component's loading conditions, material composition and geometry, as well as the specific technical requirements of the zone to be hardened.

Simulation-based workflow:

- Prediction of the required hardness profile and process parameters
- Derivation of the optimum laser beam intensity distribution and geometry
- Development of the optical design

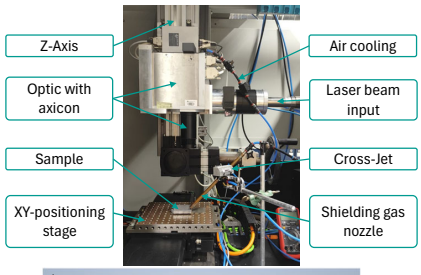


- Experimental implementation
- Generation of a laterally and axially tailored beam profile, allowing the component to be hardened in a targeted and energy-efficient manner

Sub-Project EAH Jena

Experimental setup:

- Fiber laser: ROFIN FL 015
- Wavelength: 1070 nm; Power: max. 1500 W



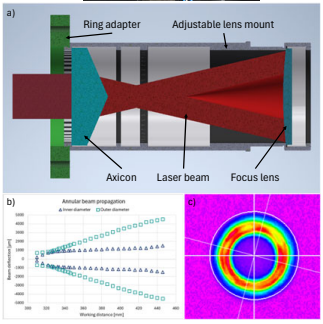
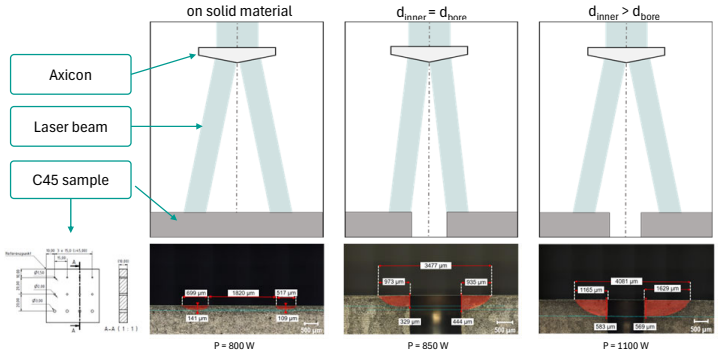


Figure: a) Cross-section of beam shaping unit with axicon; b) measured annular beam propagation; c) measured annular intensity profile

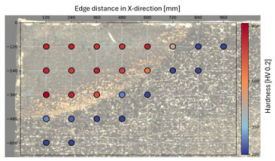
Results:

- Static processing strategies (schematic illustration) for bores using an annular beam profile, with corresponding cross-sections of hardened C45 samples:



→ Tailored laser beam shaping and offset between laser beam and bore ($d_{inner} > d_{bore}$) promote geometry-induced heat accumulation, supporting the hardening process and increasing the transformed volume by a factor of 3.3

- Vickers hardness (HV0.2) measurement of the hardened bore surface
- The visualisation demonstrates increased hardness up to 916 HV0.2 within the irradiated area compared with the surrounding base material



Outlook:

- Revision and optimisation of the optical design
  - → Homogenisation of the intensity distribution
  - → Variation of inner diameter independent from outer diameter
  - → Laser power up to 4 kW using a disc laser
  - → Collimated annular laser beam in the interaction zone
- Static and dynamic laser beam hardening using a robotic system with inverted kinematic

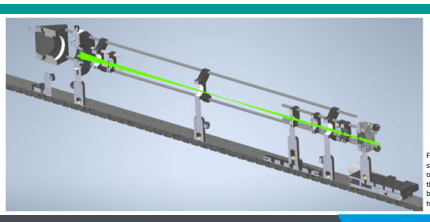


Figure: Cross-section of the optical design of the optimised beam path with two axicons

Contact:
Prof. Dr.-Ing. Jens Bliedtner
jens.bliedtner@eah-jena.de
Ernst-Abbe-Hochschule Jena
Carl-Zeiss-Promenade 2
07745 Jena

Prof. Dr. rer. nat. Robert Brunner
robert.brunner@eah-jena.de
Ernst-Abbe-Hochschule Jena
Carl-Zeiss-Promenade 2
07745 Jena

Prof. Dr. rer. nat. Tom Lahmer
tom.lahmer@uni-weimar.de
MFPA Weimar
Coudraystraße 9
99423 Weimar

The research results were obtained as part of a project funded by the Free State of Thuringia and co-financed by the European Union through the European Regional Development Fund (ERDF) (Project No.: 2024 FGR 0036).

Antibacterial surface functionalization of carbon layers through laser treatment

A. Kratsch, N. Nieher, V. Voropai, J. Döring, S. Weißmantel

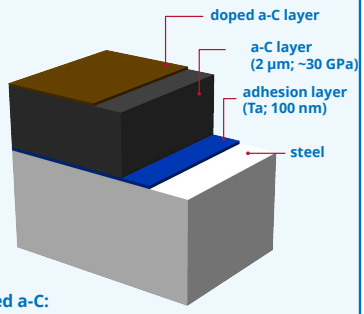
Aseptic loosening and periprosthetic infections are the main causes of revision surgery on patients with endoprosthetic joint implants. Infections alone caused 18.5% of hip-implant, 15.2% of knee implant and 14% of shoulder implant revision surgeries in 2024. This study presents laser based surface treatments which can reduce the post prosthetic infection risk. The modifications were applied to hydrogen-free hard protective amourphous carbon coatings (a-C) on steel. The a-C layer acted as an ion barrier between prosthesis and surrounding tissue as well as provide mechanical protection against the strenuous implantation process. Two strategies showed promising results this far.



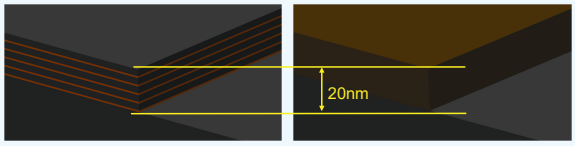
Humerus component of a shoulder prosthesis.

Doped carbon coatings (a-C)

Polished steel samples were coated via Pulsed Laser Deposition (PLD). Samples were cleaned using an Ar+ ion-beam prior to layer deposition. A KrF excimer laser source was used for the coating process. All Targets were illuminated with 6 J/cm² fluence.



Production methods of doped a-C:



Altering targets; Sub-layers statistically thinner than than one atom layer

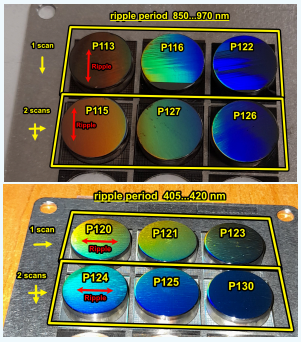
Target consists of an amalgum or material mixture; results in homogenous doped layer

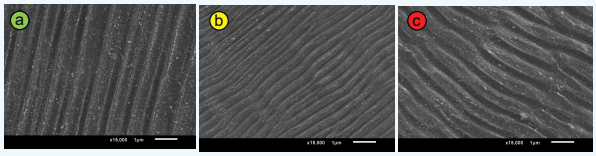
Laser Induced Periodic Self-organizing Surface Structures (LIPSS; "Ripple")

Ripple are structured via 190fs laser pulse irradiation. The beam was steered across the a-C layer surface via a scanner module. Two different central wavelengths were tested, using the following parameters:

λ = 1030 nm	λ = 514 nm
w_0 = 20,3 µm	w_0 = 14,5 µm
H_0 = 1,1 J/cm²	H_0 = 1,7 J/cm²

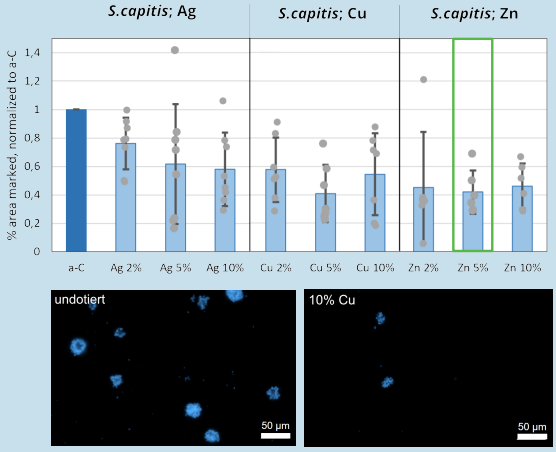
Different processing parameters influenced ripple morphology and therefore their affect on bacterial growth.



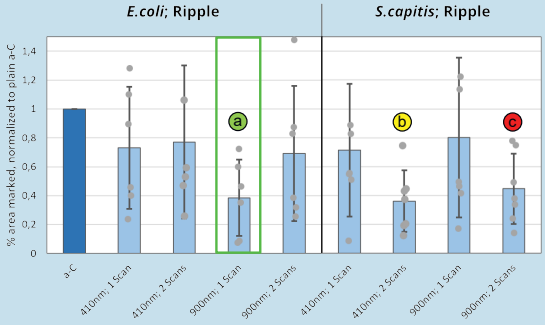


Antibacterial Effects

Prepared samples were sterilized and incubated for 24h with *E.coli* or *S.capitis* cultures. After washing, fixation and DAPI-staining, bacterial colonization was analyzed via fluorescence microscopy and subsequent image analysis.



Reduction of S.capitis colonization due to a 10% Cu-doped a-C coating.



Copper and zinc doped a-C coatings showed a significant antibacterial effect on *S.capitis*, whereas ripple with 900 nm period significantly affected *E.coli*. Bacterial colonialization could be reduced by roughly 50% in both cases. A combined surface treatment is suspected to be effective against both strains. This is subject to further investigations.

Laserinstitut Hochschule Mittweida
Technikumplatz 17, 09648 Mittweida
Alexander Kratsch
kratsch@hs-mittweida.de | +49 3727 58 1443
www.laser.hs-mittweida.de

Gefördert durch:
Bundesministerium für Wirtschaft und Klimaschutz
aufgrund eines Beschlusses des Deutschen Bundestages
ZIM Zentrales Innovationsprogramm Mittelstand

Generation of laser-induced shock waves in concrete structures for analytical applications and material evaluation

Manuel Pfeiffer, Peter Lickschat, Aaron Thriemer, Ertac Celik, Jörn Hübelt, Steffen Weißmantel

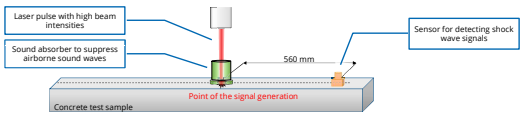
The measurement method introduced here is a newly developed opto-acoustic in-situ measurement technique for the non-destructive and non-contact assessment of concrete structures. It can be used to characterize material quality and aging, as well as to detect defects. This method is based on the non-contact interaction of high-energy, short laser pulses with the material surface to generate laser-induced shock wave signals, and on the non-contact detection of the resulting vibration patterns — which are influenced by the material properties — using Laser-Doppler-anemometry. The frequency-dependent phase-velocity can then be calculated from the acquired data using wave field transformation and the "Multichannel Analysis of Surface Waves" (MASW) method. This will allow the material properties to be characterized afterwards.

Introduction:

- The goal of the research was to generate laser-induced shock wave signals in concrete components for subsequent opto-acoustic applications.
- The studies focused on signal level and its relationship to system configuration.
- The research was based on a SpitLight solid-state laser system (parameters: wavelength 1064 nm, pulse energy up to 2500 mJ, pulse duration 6–8 ns)
- A single-point laser vibrometer (model VFX VibroFlex QTec) was used to measure the vibration patterns using Laser-Doppler-anemometry.

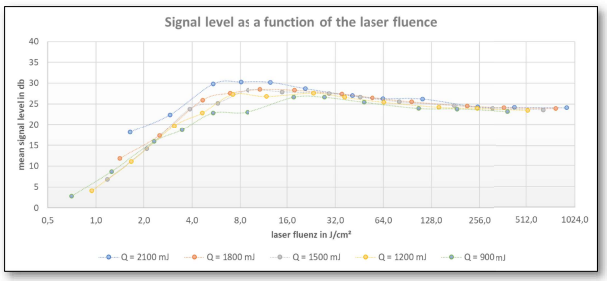
Basics of the laser-induced shock waves:

- The absorption of high-energy laser pulses combined with short laser pulse durations leads to an explosive plasma formation on the material's surface.
- The plasma expansion generates a counteracting force impulse, resulting in a shock wave within the test material that propagates as a vibration field.
- To investigate the signal levels of the shock waves, the following test setup was used, which included a sound absorber to suppress the airborne sound waves generated secondarily by the plasma:

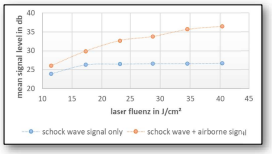


Results of the signal level studies:

- The mean signal level is determined from the frequency-dependent signal-to-noise ratio data of the experimentally measured laser-induced shock wave signals.

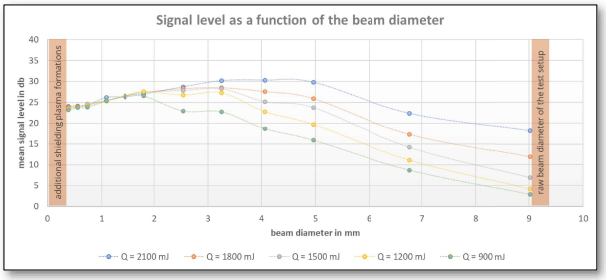


- In general, higher pulse energies can result in higher signal levels, but this depends heavily on how the energy is distributed across the material's surface.
- An optimal surface energy density — resulting in the highest possible signal levels during laser-induced signal generation on concrete — is achieved at fluences ranging from 6 J/cm² to 18 J/cm².
- Higher fluence values do not result in higher signal levels, because the energy from the laser pulse is shielded by the plasma, thereby amplifying only the secondary airborne sound waves.



Results related to the optical setup:

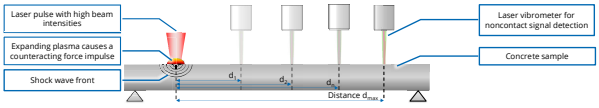
- Energy is distributed by changing the beam diameter on the material surface, either through defocusing or by changing the focal length of the optics.
- There is an optimal diameter range for the generation of laser-induced shock waves, and changing the beam diameter is only useful within certain limits:



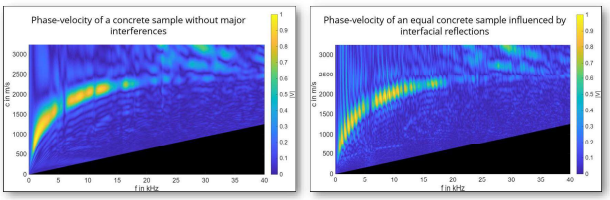
- If the beam diameter is set too low, the resulting high energy densities lead to the formation of an additional shielding plasma in the air above the material surface.

Determination of the frequency-dependent phase-velocity:

- Based on measured shock wave signals, the frequency-dependent phase-velocity can be determined using the "Multichannel Analysis of Surface Waves" (MASW) method, which is based on a wave-field transformation.
- The setup for determining the phase velocity requires measurements of the signal at multiple distances d:



- As an example of an application, the frequency-dependent phase-velocity profile can be used to non-destructively detect hidden interfaces of defects or cracks in the concrete material using pattern recognition:



Acknowledgment:

- The study was funded by the Free State of Saxony and the European Union as part of the "VIVA-SAX - Validierung von Innovationen und Verwertungen Sachsen" validation program.

Co-funded by the European Union
Freistaat SACHSEN
This project is co-financed from tax revenues on the basis of the budget adopted by the Saxon State Parliament.

Laserinstitut Hochschule Mittweida
Technikumplatz 17, 09648 Mittweida
Dipl.-Ing. (FH) Manuel Pfeiffer
pfeiffer@hs-mittweida.de
www.laser.hs-mittweida.de

Laserinstitut Hochschule Mittweida LHM

ukpiño

Gefördert durch: Bundesministerium für Forschung, Technologie und Raumfahrt

Ernst-Abbe-Hochschule Jena
University of Applied Sciences

Selective Laser Activation and Metallization of Natural Fiber Textiles

Robert Schmidt[1], Andreas Knauft[1], Andrea Barz[1], Jens Bliedtner[1], Marcel Bäuml[2], Andreas Ludwig[2], Henrik Banse[3], Jan Langebach[3]

[1]Ernst-Abbe-University of Applied Sciences Jena, Carl-Zeiss-Promenade 2, 07745 Jena
[2]Thorey Gera Textilveredelung GmbH, Lange Str. 71, 07551 Gera
[3]JENOPTIK Automatisierungstechnik GmbH, Konrad-Zuse-Straße 6, 07745 Jena

Objectives

Conductive textiles are gaining importance in wearable electronics [1, 2], with applications in healthcare, sports, protective clothing, and entertainment [3]. This work investigates the selective metallization of natural fiber-based textiles using an ultrashort-pulse laser (1030 nm, 500 fs). Laser irradiation locally modifies the textile surface, enabling activation through palladium seeding in a $PdCl_2$ solution. Copper is then deposited selectively on the laser-treated areas using an electroless $CuSO_4$-based process, forming selective structures. This approach has mainly been studied on polymers [4] and synthetic textiles [3]. This work extends the process to natural fiber-based cotton textiles. It is investigated how laser parameters, chemical conditions, and textile weave structures of different cotton types influence metallization quality. The aim is to produce copper structures with small feature widths, well-defined geometries, good adhesion, and low electrical resistance for E-Textile applications.

Process Chain

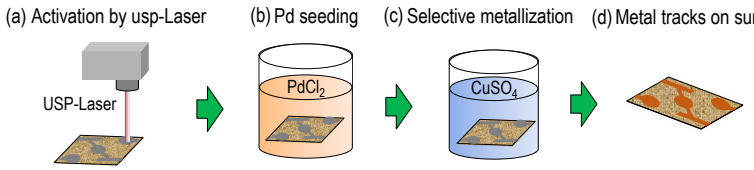


Fig. 1: Process chain for selective metallization of Natural Fibre Textiles (a) laser activation of the surface, (b) seeding with $PdCl_2$, (c) selective metallization with $CuSO_4$ and (d) conductive structures on the textile surface

Influencing Factors

- Laser & Scan Parameters: wavelength λ, pulse duration t_p, repetition rate RR, focal spot diameter d_F, fluence F_L, pulse distance d_p, line distance d_L, number of scan passes z
- Chemical Parameters: Temperature, concentration of $PdCl_2$ and $CuSO_4$, dwell time
- Material Properties
- Textile Structure

Material

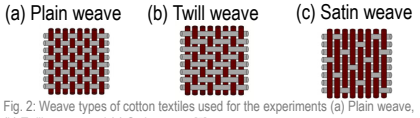
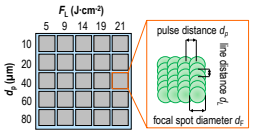


Fig. 2: Weave types of cotton textiles used for the experiments (a) Plain weave, (b) Twill weave, and (c) Satin weave [5]

Process Parameters

Laser parameters
- λ = 1030 nm
- t_p = 500 fs
- RR = 25 kHz



Chemical Parameters
- $PdCl_2$: 2 g/L, 80 °C 20 min 100 ml
- $CuSO_4$: 47 °C, 20 min, 300 ml

Results

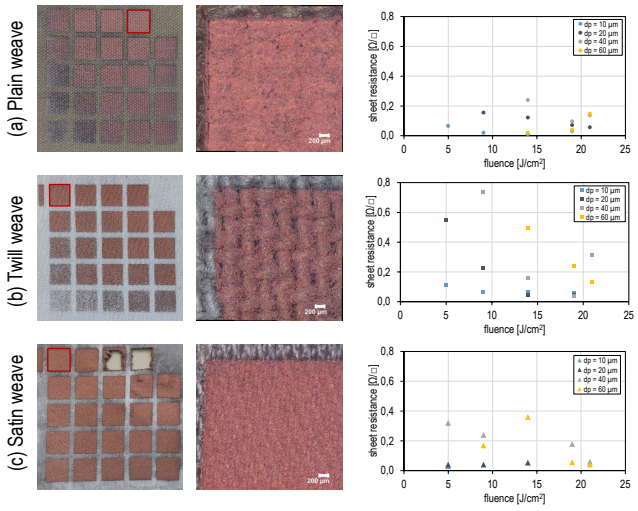


Fig. 3: Metallization results and electrical resistance for different laser parameters across three weave types of natural fiber-based textiles: (a) Plain weave, (b) Twill weave, and (c) Satin weave

Plain weave
- Stiff and robust substrate, tolerates high energy inputs
- Narrow Process Window
- Small mesh size

Twill weave
- Coarser Structure
- Interstitial voids risk disrupting trace continuity and reducing pattern resolution

Satin weave
- Thin substrate, lower thermal stability
- Broader Process Window, higher selectivity

General
- Plain & satin weaves: lower sheet resistance than twill (due to coarser twill structure)
- Discoloration observed on all substrates

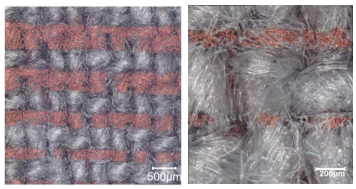


Fig. 4: Light microscopy images of the minimum achievable line width of twill weave cotton for F_L = 14 J/cm², d_P = 40 µm

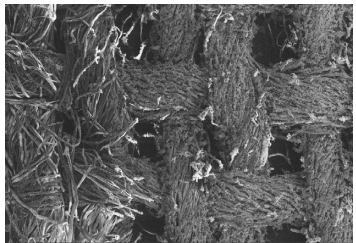


Fig. 5: Scanning electron microscopy (SEM) image of the transition zone between the selectively metallized region and the surface without laser activation (Twill weave)

Conclusion

In this study, selective metallization was achieved on USP-laser-activated cotton textiles. Different weave structures, ranging from twill to satin, exhibited processing windows with homogeneous metallization, although satin was more sensitive to high laser energy inputs. Pattern resolution was primarily determined by the mesh size and gaps between individual threads, while the metallized structures exhibited low electrical resistance. However, chemical bath treatment can cause discoloration of the natural fiber substrate. Overall, selective metallization via USP laser activation offers promising potential for E-Textile applications.

References

[1] X. Liu et al. (2010): „Polyelectrolyte-Bridged Metal/Cotton Hierarchical Structures for Highly Durable Conductive Yarns"; ACS Applied Materials & Interfaces, pp. 529-535.
[2] T. J. Kang et. al. (2010): "Electromechanical properties of CNT-coated cotton yarn for electronic textile applications"; Smart Materials and Structures, vol. 20, no. 1.
[3] J. Bliedtner et. al (2024): "Precision laser metallization of textile surfaces for advanced smart fabric applications"; Trends in Textile Engineering & Fashion Technology, vol. 10, no. 3.
[4] M. Seiler et. al (2020): "Laser beam activation of polymer surfaces for selective chemical metallization"; Procedia CIRP, vol. 94, pp. 891 – 894.
[5] Barth & Könenkamp Seiden, "Bindungsarten"; Seidenratgeber. Available: https://www.barth-seiden.de/seiden-ratgeber/bindungsarten/.; 21.04.2026.

Kontakt
Prof. Dr.-Ing. Jens Bliedtner
Jens.Bliedtner@eah-jena.de
Ernst-Abbe-Hochschule Jena
Carl-Zeiss-Promenade 2
07745 Jena

M.Eng. Robert Schmidt
Robert.Schmidt@eah-jena.de
Ernst-Abbe-Hochschule Jena
Carl-Zeiss-Promenade 2
07745 Jena

This article presents results from the research and development project "UKPiño" (reference number 03RU2U033I), funded by the German Federal Ministry of Research, Technology and Space (BMFTR). The authors are responsible for the content of the publication.

AG bliedtner
Laser | Optik | 3D-Druck

Evaluating the Weather-Dependent Reliability of a Scanning Doppler Wind Lidar

Jan Shames[1], Julian Leiber[1], Jeffrey D Thayer[2], Clémence Dubois[1], Norman Wildmann[2]

Overview

Motivation

- Scanning Doppler wind lidars require substantial logistical and financial effort.
- Their measurement range and reliability depend on local atmospheric conditions.
- Quantifying these limitations supports campaign planning and the interpretation of long-term wind observations.

Objective

- Assess the long-term, weather-dependent performance of a scanning Doppler wind lidar and identify the environmental conditions associated with reduced data quality.

→ **Further goal:** Contribute to improved wind-turbine efficiency through reliable wind-field measurements.

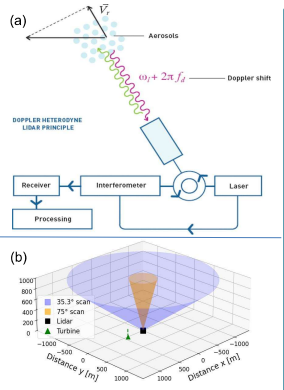


Fig. 1: (a) Doppler wind lidar principle [1]. (b) Measurement setup.

Instrument

- Pulsed Leosphere WindCube 200S Doppler wind lidar.
- 200 ns pulse length and 10 kHz pulse repetition.
- VAD scans at 35.3° and 75° elevation.



Dataset

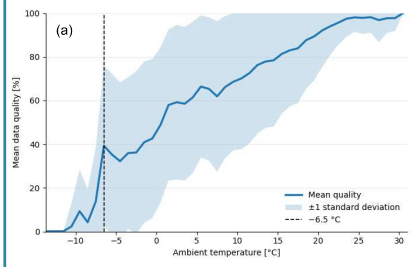
- WiValdi research wind farm, coastal northern Germany.
- January 2021–March 2025, total scans: 1.3 million.
- Analysis limited to altitudes up to 1 km (boundary-layer limit for aerosol signal).

Methodology

- Radial velocities accepted for signal-to-noise ratio values from −25 to 0 dB.
- Data quality defined as percentage of valid range gates per scan.
- Data from both scan angles were combined because their quality was nearly identical.
- Evaluated variables: pressure, temperature, wind speed/direction, relative humidity, and rainfall.

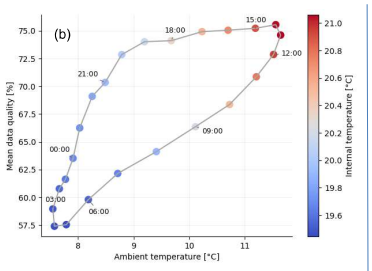
Results

Fig. 2: Temperature dependence of data quality. (a) Mean quality in 1°C bins with ±1 standard deviation and the −6.5°C threshold. (b) Daily hysteresis between ambient temperature and data quality. Point color indicates the corresponding internal temperature. (c) Hourly temperature deviations from the mean and data quality in comparison.



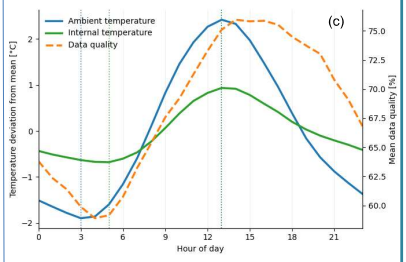
Temperature dependence

- Data quality increases with temperature.
- Almost no valid data below -11.5°C.
- Sharp increase from 14% to 39% between -7.5°C and -6.5°C.



Temperature hysteresis

- Higher evening than morning data quality at the same temperature.
- Ambient and internal temperatures alone are insufficient to explain lidar data quality.
- Additional factors are likely needed to explain the observed hysteresis.



Daily temperature response

- Morning: internal temperature and data quality reach their minima about 2 h after ambient temperature.
- Afternoon: availability peaks 2 h after temperature maxima.
- Internal temperature explains part of the morning shift.

Humidity and saturation

- Significant data quality drop near 0°C dew-point depression.
- Strongest effect under cold, near-saturated conditions.
- Likely linked to condensation on the optics.

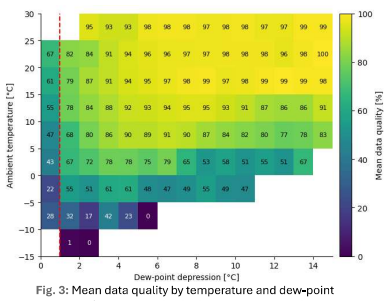


Fig. 3: Mean data quality by temperature and dew-point depression; dashed line indicates near-saturation.

Rainfall effects

- Clear data quality drop from no rain to rain above 0°C.
- At high temperatures, data quality decreases more strongly with increasing rainfall intensity.
- Below 0°C (purple curve), data quality increases with rainfall intensity; possibly due to enhanced backscatter from frozen precipitation (limited data above 1 mm/h).

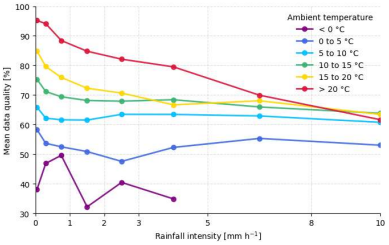


Fig. 4: Mean data quality by rainfall intensity and temperature range.

Conclusion

- Temperature seems to be the main driver of lidar data quality.
- Data quality decreases strongly under cold and near-saturated conditions.
- Rainfall effects depend on temperature.
- Pressure and wind speed have only secondary influence (not shown).

→ Lidar positioning should consider local climate, as warmer, drier conditions improve data quality.

Outlook

- Hysteresis not fully explained.
- Additional influencing factors to investigate (mixing layer height, turbulence).

Deutsches Zentrum DLR für Luft- und Raumfahrt

Contact: [1]**DLR - Institute of Data Science** | Department Data Analysis and Intelligence | Jena
Jan Shames | E-Mail: jan.shames@dlr.de

[2]DLR – Institute of Atmospheric Physics | Oberpfaffenhofen

Poster reference:
[1] Leosphere, WindCube Scan Hardware and Maintenance User Manual, Doc. MZ12326EN-E, 2021.

Leibniz Ferdinand Braun Institut

Ferdinand-Braun-Institut
Leibniz-Institut für Höchstfrequenztechnik
Gustav-Kirchhoff-Straße 4, 12489 Berlin

Tel +49 30 6392-3956 Fax +49 30 6392-2602
nils.werner@fbh-berlin.de www.fbh-berlin.de

With funding from the:

Federal Ministry of Research, Technology and Space

APECS

Hybrid Laser Sources in the Yellow-Green Spectral Range: Tailored Light for Bio-Medical Applications

Nils Werner, Alexander Sahm, David Feise, Gunnar Blume, Katrin Paschke

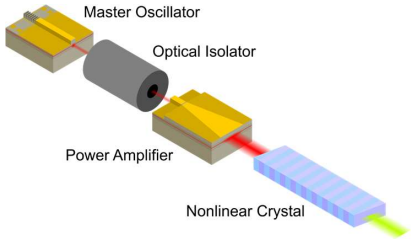
Ferdinand-Braun-Institut, Leibniz-Institut für Höchstfrequenztechnik
Gustav-Kirchhoff-Straße 4, 12489 Berlin, Germany

Motivation and Challenges

- Laser sources in the yellow-green spectral range are demanded in various applications in life sciences and medicine:
  - Fluorescence microscopy (e.g. STED)
  - Ophthalmology
  - Dermatology
- No direct-emitting diode lasers available in this spectral range
  - Advantages of diode lasers (efficiency, modulation capability, compactness) remains untapped in these applications

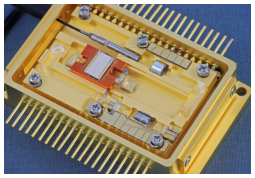
Our Approach

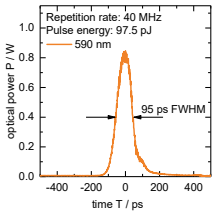
- Tailored near-infrared-emitting diode lasers
  - Master Oscillator Power Amplifier concept
  - High output power at nearly arbitrary wavelengths
    - E.g.: 1122 nm, 1154 nm, 1180 nm
- Second harmonic generation
  - Nonlinear crystals convert emission to yellow-green spectral range: 561 nm, 577 nm, 590 nm



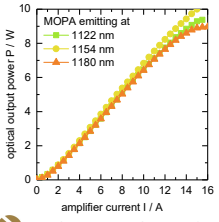
Pulsed Laser Sources

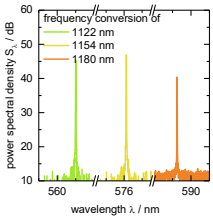
- Fully integrated module with MOPA, nonlinear crystal and fiber output
  - Pulsed emission by gain switching of Master Oscillator
  - High repetition rates up to 80 MHz, pulse lengths around 100 ps
  - Concept can realized at various wavelengths e.g. 561 nm or 590 nm





Left: Hybrid-integrated laser source for pulsed emission at 590 nm.
Right: Pulse shape of the 590 nm emission.

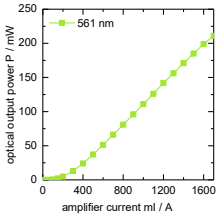


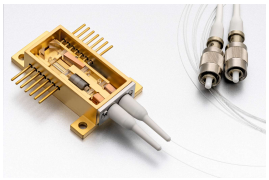


Top: Schematics of Master Oscillator Power Amplifier (MOPA) and second harmonic generation (SHG). Bottom: Near infrared output characteristics of MOPAs and spectra of converted light in the yellow-green spectral range.

CW Laser Sources

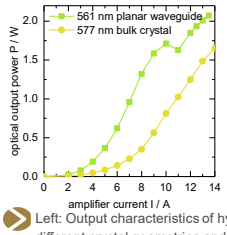
- Highly compact module with power amplifier and nonlinear crystal
  - PM fibers for external Master Oscillator input and SHG output
  - Medium power levels up to 200 mW
  - Operation with reduced periphery and control loops

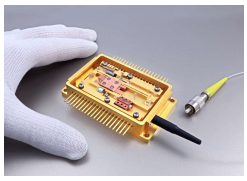




Left: Output characteristics of fiber-coupled amplifier module at 561 nm.
Right: Hybrid-integrated amplifier module with PM-fiber ports.

- Fully integrated module with MOPA and nonlinear crystal
  - Optional fiber output
  - High optical output power up to 2 W
  - Nonlinear crystal geometries tailored to the application





Left: Output characteristics of hybrid integrated laser modules with different crystal geometries and emission wavelengths.
Right: Hybrid module with planar waveguide crystal and fiber output.

Acknowledgement

- Federal Ministry of Research, Technology and Space
- APECS is co-funded by the Chips Joint Undertaking and national funding authorities of Austria, Belgium, Finland, France, Germany, Greece, Portugal, Spain, through the Chips for Europe Initiative

Contact

Laser Modules Lab
Dr. Katrin Paschke
katrin.paschke@fbh-berlin.de
www.fbh-berlin.com/research/photonics/laser-modules

E. Hofbauer, R. Kometer, HOFBAUER OPTIK Mess- & Prüftechnik

OPTIK · MESS- UND PRÜFTECHNIK
VERTRIEB · BERATUNG · TRAINING

HOFBAUER

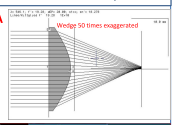
Optimized Blocking on Mandrel
No Centering Error, Polishing Error and 'slope error' on Aspheres

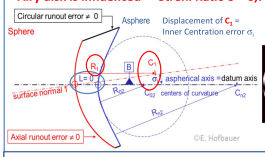
Motivation: Problems with and on Aspheres

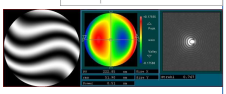
- Partly high scrap rates in **Aspheres production** -> 'Inner Centration'
- **Mounting of semi-finished asphere on mandrel** as a challenge
- No fast, easy and precise measurement process for Centration Error
- Decenter on mounted lens leads to Polishing and Slope Errors

Laser Beam Error on High NA-Lens (0,5) with Centration Error 0,3'

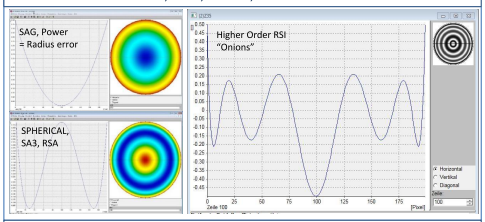
- A small wedge of **0.3 arcmin** causes significant **COMA**
- First order COMA 0.32 lambda PV@633 nm (223 nm) or 0.08 lambda rms (52 nm)
- **Airy disk is influenced -> Strehl Ratio S = 0,77**





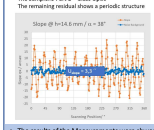


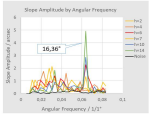
Gobal form Errors SAG, ASTI, COMA, RSI



Local form Errors as Mid-Spatial-Frequency Errors (MSFE)

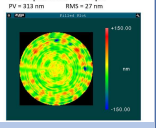
The slope measurement in sagittal direction in the outer zone of the aspheric lens is showing a periodic structure.





The Fourier-Transform reveals a significant periodic structure at 16,36°.

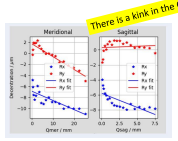
After integration and interpolation we are able to derive a 2D-Surface plot of the SUT. The clearly visible „spokes" are a typical remain of the grinding process (**)

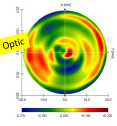


- The results of the Measurements were shwon at the IWXM (2022)
** Olga Kuksa et al., "On the metrology of MSF errors after grinding," Proc. SPIE 10742, Optical Manufacturing and Testing XII, 107420X (14 Sept. 2018)

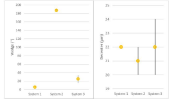
Effect of Local Irregularities (f.e. local Coma) on Centration Results *

The point-wise measurement of the decentration along the asphere axis can not be fitted by one straight line. This indicates a change in tilt depending on the zone of measurement. This effect is called a *„Kink in the Optic"*.





This local coma is described as falling in between classical form and decenter specifications, which becomes evident when comparing different measurement techniques, that show strong differences in reported wedge angle, depending on the number of measurement points.



The detailed surface measurement shows a strong asymmetric center artifact – i.e. local coma.

T8423	Anph. Axis 1 vs. Anph. Axis 2	
	Wedge (°)	Uncertainty
System 1	0,0	0
System 2	0,0	0
System 3	0,0	0

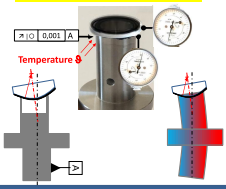
Decenter (µm)	Uncertainty
25	5
25	5
25	5

* M. Knobl, J. DeGroote Nelson, et al. Edmund Optics Inc.: High Order Surface Artifacts on Aspheres and their Interpretation in Metrology and Tolerancing, EOSAM 2024

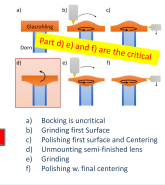
Problems at Manufacturing Process of Aspheres

- Inner decentration results during grinding and polishing process
- No good equipment is reliable for cementing Aspheres
- Vertex of lower side is not measureable by dial gauge
- Axial and circular runout of mandrel has to be < 1 µm
- Painting/ Purple tape has to have an even thickness < 1 µm
- Dial gauges on rough cylinder barrel is imprecise > 1 µm
- Blocking lens by temperature may cause decentration
- **NEW: HD-Chuck on Machine Spindle Axis C is a great Problem** circular runout: up **to 4 µm**, tilt angle runout up to **30 arcsec**

5 errors - to be avoided

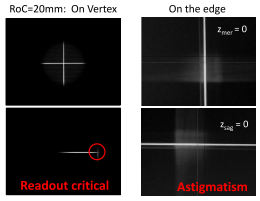


Manufacturing Aspheres on stem: Because it is the best way -> Accuracy



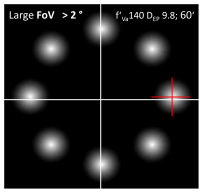
Vignetting Field Stop VFS and Measurement Process on Aspheres

Problems @Auto Collimator AC:
Different Apertures, Focussing lens or RoC

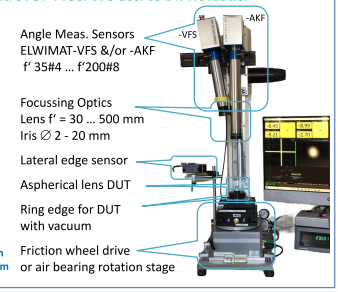


- Small Aperture ↓-> small FoV ↓ -> Only one direction of
- Small WD ↓ ---> Vignetting ↑ image is measurable
- -> small DoFocus: 0,1 ... 1 mm ↓ -> critical Depth of Focus ↓

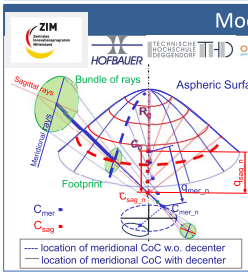
The Solution @Vignetting Field STOP Proc. VFS acc. to Dr. Hofbauer

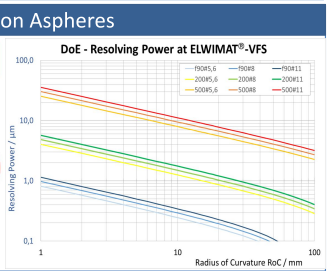


- Small Aperture -> large FoV ↑ up to 10°
- Large Working distance WD ↑ up to 0,5m
- High depth of Fokus f' 140 F#11: ± 100mm



Model and Design of Experiment on Aspheres





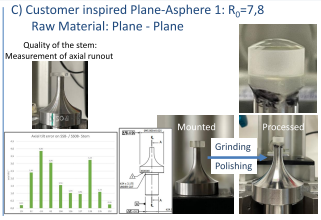
Our Test Models and lenses to be blocked: grinded plane Surface on top

A) Developing a Manipulator
- Mounting and glueing independent from the accuracy of stem
- Sensitivity < 1 µm and 5 arcsec

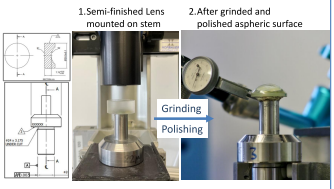
B) Develope a direct drive HD-25
- Circular Runout << 1µm

C) Customer inspired Plane-Asphere 1: R_0=7,8
Raw Material: Plane - Plane

Quality of the stem: Measurement of axial runout



D) Customer inspired Sphere – Asphere: R_0=13 mm
Raw Material: Plane - Spheric



Centration Measurement Results by NEW controlled Blocking on Stem Process

- ✓All lenses were successfully measured On and Off Stem
- ✓Spheric lens was measured with MCM friction wheel drive
- ✓ Single Aspheric lenses were measured with new ACM
- ✓ Grinding Chuck seems to have axial runout ≈ 3.5 µm

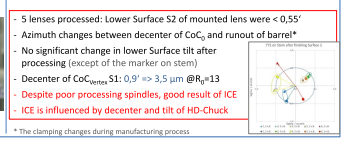
Measure circular runouts of finished Asphere on stem and inner Centration Error ICE

No.	After Mounting		After Processing - On Stem			- Off Stem
	Wedge*	S2	S2= plane	S1= Asphere CoC_0		ICE Inner Centration
1	0,6'	0,04'	n.A.**	4,0 µm	1,7'	1,79'
3	0,77'	0,15'	0,21'	3,7 µm	1,6'	1,82'
4	0,82'	0,14'	0,07'	0,8 µm	0,35'	0,83'
5	0,68'	0,6'	0,60'	1,9 µm	0,8'	1,28'
6	0,71'	0,23'	0,22	2,8 µm	1,2'	3,06'



- 5 lenses processed
- Lower Surface of mounted lens < 0,6'
- Decenter of CoC_0 up to 1,7' => 4 µm @R_0 = 7,8
- HD-Chucks on Manufacturing Spindles seems to be ‚Out of Order'
- Despite poor processing spindles, good result of ICE

* Measured on Semi finished Lens
** not measurable because full of glue on back side



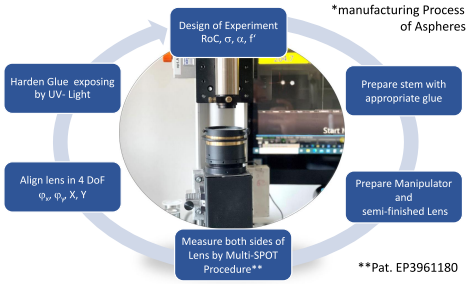
No	After Mount	After Processing - On Stem		- Off Stem
	S2 R=12	S2 R 12	Asph. CoC_0	ICE
1	0,3'	0,48'	0,9'	1,34'
3	0,48'	0,45'	0,28'	0,56'
4	0,55'	0,52'	0,21'	1,03'
5	0,2'	0,3'	0,76'	1,10'
6	0,3'	0,22	0,68'	1,04'

- 5 lenses processed: Lower Surface S2 of mounted lens were < 0,55'
- Azimuth changes between decenter of CoC_0 and runout of barrel*
- No significant change in lower Surface tilt after processing (except of the marker on stem)
- Decenter of CoC_{Vertex} S1: 0,9' => 3,5 µm @R_0=13
- Despite poor processing spindles, good result of ICE
- ICE is influenced by decenter and tilt of HD-Chuck

* The clamping changes during manufacturing process

Pat. Pending ... Mounting Process Step d)*

*manufacturing Process of Aspheres



**Pat. EP3961180

Summary

The Vignetting Field STOP-Procedure
- Large field of view (FoV) and large working distance (WD)
- Manipulator allows high precision in independent DoF:
- 0,1 µm < dx, dy < 1 µm and 0,05 < sigma < 0,5'
- Fast Process time to process < a few minutes
- ICE is influenced by decenter and tilt of HD-Chuck on C-axis

Outlook

Following Activities are in progress
- Completing and optimize Software evaluation
- Integration of DoE-Calculation in Software Module
- Further Customers Trials for best Quality even Spherical Surface on Top: Spheric – Spheric
- Next Grinding and Polishing with better HD Chuck

References and Acknowledgement

(1) E. Hofbauer: Verfahren und Messvorrichtung zur berührungslosen Messung von Winkeln oder Winkeländerungen an Gegenständen Veröffentlichungs-Nr.: EP 1636542 B1, 2004
(2) E. Hofbauer, M. Lenz: Vignettierung als physikalisches Messprinzip zur zweidimensionalen Winkelmessung; tm-Technisches Messen, 75 (3), 153-167, 2008
(3) E. Hofbauer: Deflectometric acquisition of large optical surfaces "DaOS" using a new physical meas. principle: vignetting field stop procedure, Proc. of SPIE Vol. 100090A-1, 2016
(4) R. Kometer, E. Hofbauer, „Fast and reliable in-situ measurements of large and complex surfaces using a novel deflectometric device", Proc. SPIE 10829, Aug. 2018
(5) E. Hofbauer, R. Kometer, "A new approach to surface shape and centration measurement on aspheres with the new V-SPOT technology, Proc. SPIE. 11171, 2019

Autor	Anschrift
Alasgarzade, Namig	Friedrich-Schiller-Universität Jena namig.alasgarzade@uni-jena.de
Bischoff, Christian	TOPAG Lasertechnik GmbH Bischoff@topag.de
Börner, Richard Prof. Dr.	Hochschule Mittweida richard.boerner@hs-mittweida.de
Brückner, Frank Prof. Dr.	Fraunhofer-Institut für Werkstoff- und Strahltechnik IWS frank.brueckner@iws.fraunhofer.de
Büttner, Sebastian	Hochschule Mittweida buettner@hs-mittweida.de
Deckert, Finn-Merlin	CiS Forschungsinstitut für Mikrosensorik GmbH fdeckert@cismst.de
Dienerowitz, Maria Prof. Dr.	Ernst-Abbe-Hochschule Jena maria.dienerowitz@eah-jena.de
Fürch, Elise	Fraunhofer-Institut für Angewandte Optik und Feinmechanik IOF elise.fuerch@iof.fraunhofer.de
Gillner, Arnold Prof. Dr.	Rheinisch-Westfälische Technische Hochschule Aachen arnold.gillner@llt.rwth-aachen.de
Güpner, Michael	Ernst-Abbe-Hochschule Jena michael.guepner@eah-jena.de
Hofbauer, Engelbert Dr. Ing.	HOFBAUER OPTIK MESS- UND PRÜFTECHNIK info@hofbauer-optik.de
Klenke, Arno	Helmholtz-Institut Jena A.Klenke@hi-jena.gsi.de
Kratsch, Alexander	Hochschule Mittweida kratsch@hs-mittweida.de
Kühn, Markus	Ernst-Abbe-Hochschule Jena markus.kuehn@eah-jena.de
Lehmann, Paul	Hochschule Mittweida lehmann6@hs-mittweida.de
Limpert, Jens Prof. Dr.	Friedrich-Schiller-Universität Jena jens.limpert@uni-jena.de
Mekle, Dario	TRUMPF Laser- und Systemtechnik SE dario.mekle@trumpf.com
Morgner, Uwe Prof. Dr.	Leibniz Universität Hannover morgner@iqo.uni-hannover.de
Münch, Marcella	Friedrich-Schiller-Universität Jena Marcella.muench@uni-jena.de
Munteanu, Toni	Innovent e.V. t.munteanu@innovent-jena.de
Nodop, Dirk Dr.	Günther Köhler Institut für Fügetechnik und Werkstoffprüfung GmbH (ifw Jena) dnodop@ifw-jena.de

Autor	Anschrift
Olbrich, Markus	Hochschule Mittweida molbrich@hs-mittweida.de
Pfeiffer, Manuel	Hochschule Mittweida pfeiffer@hs-mittweida.de
Prévost, Vincent	Laser 2000 GmbH v.prevost@laser2000.fr
Rudolph, Kris Dr.-Ing.	PRIMES GmbH k.rudolph@primes.de
Rupf, Vincent	Hochschule Mittweida rupf@hs-mittweida.de
Scheffler, Jonas	Technische Universität Ilmenau jonas.scheffler@tu-ilmenau.de
Schmidt, Thomas	Günther Köhler Institut für Fügetechnik und Werkstoffprüfung GmbH (ifw Jena) tschmidt@ifw-jena.de
Schmidt, Robert	Ernst-Abbe-Hochschule Jena Robert.Schmidt@eah-jena.de
Schröder, Daniel Dr.	Leibniz-Institut für Photonische Technologien e.V. (Leibniz-IPHT) daniel.schroeder@uni-jena.de
Seiler, Michael	SCHOTT Technical Glass Solutions GmbH michael.seiler@schott.com
Shames, Jan	Deutsches Zentrum für Luft und Raumfahrt jan.shames@dlr.de
Stelzig, Carl	LCP Laser-Cut-Processing GmbH carl.stelzig@lcpgmbh.de
Werner, Ekkehard Dr.	Jenoptik Optical Systems GmbH ekkehard.werner@jenoptik.com
Werner, Nils Dr.	Ferdinand-Braun-Institut, Leibniz-Institut für Höchstfrequenztechnik (FBH) nils.werner@fbh-berlin.de